SURFACE REDUCTIVE CAPACITY OF CARBON NANOMATERIALS AFTER VARIOUS HEATING AND AGING PROCESSES

A Thesis

by

CHUNGHOON LEE

Submitted to the Office of Graduate Studies of
Texas A&M University
in partial fulfillment of the requirements for the degree of

MASTER OF SCIENCE

August 2011

Major Subject: Mechanical Engineering

SURFACE REDUCTIVE CAPACITY OF CARBON NANOMATERIALS AFTER VARIOUS HEATING AND AGING PROCESSES

A Thesis

by

CHUNGHOON LEE

Submitted to the Office of Graduate Studies of
Texas A&M University
in partial fulfillment of the requirements for the degree of

MASTER OF SCIENCE

Approved by:

Chair of Committee,	Bing Guo
Committee Members,	Manuel P. Soriaga
	Xinghang Zhang
Head of Department,	Dennis O'Neal

August 2011

Major Subject: Mechanical Engineering

ABSTRACT

Surface Reductive Capacity of Carbon Nanomaterials
after Various Heating and Aging Processes. (August 2011)
Chunghoon Lee, B.E., Korea Military Academy
Chair of Advisory Committee: Dr. Bing Guo

Understanding the toxicity of carbon nanomaterials, such as carbon nanotubes and graphenes, is important for the development of nanotechnology. Studies have shown that surface redox capability is an important factor for toxicity of carbon nanomaterials. We have measured the surface reductive capacity for a number of carbon nanomaterials in previous studies, but the effects of various engineering processes on surface redox capability have not been investigated until this study.

In this study, commercially available carbon black, carbon nanotubes, standard reference materials, fullerenes, graphenes and acetylene soot generated in the lab were used. The carbon nanomaterials were subjected to heating at various temperatures in various atmospheres up to 500 ˚C, and soaking in water at room temperature under various atmospheres, and weathering in the powder form at room temperature under various atmospheres. The redox capability of the carbon nanomaterials was quantified in terms of the reductive capacity towards Fe^{3+} ions (RCFI). The RCFI values of the as-received nanomaterials and that of the nanomaterials after various treatments were compared. The carbon nanomaterials were also characterized using x-ray photoelectron

spectroscopy (XPS), for understanding the surface chemistry mechanisms of RCFI and the effects of various treatments.

In general, heating induced a significant increase in RCFI, regardless of the atmosphere under which the nanomaterials were heated. On the other hand, aging in O_2-containing atmospheres brought about significant decrease in RCFI, either in water suspension or in the powder form. Water vapor enhanced the aging effect of O_2. CO_2 was found to affect the RCFI and the aging of carbon nanomaterials. The extent of RCFI change due to heating or aging was dependent on the type of material.

According to the XPS results, the RCFI of some carbon nanomaterials such as carbon black may be correlated with the C-O surface functional groups. However, the definitive correlation between the oxygen-containing surface functional group and RCFI for all carbon nanomaterials couldn't be determined by the XPS result. This indicates that the RCFI changes of carbon nanomaterials after treatments mainly derived from the factors such as the active sites of edges other than the oxygen-containing surface functional group changes as other studies show. This suggests that the RCFI measurement cannot be replaced by XPS analysis.

The effects of heating and aging on RCFI, and more generally the surface redox capability of carbon nanomaterials, reveals that various engineering and environmental processes may significantly change the toxicity of carbon nanomaterials. The findings of this study suggest that it is important to take into account the effects of engineering and environmental processes when assessing the toxicity of carbon nanomaterials.

DEDICATION

To my God, and my lovely wife, Hana. Her support was my motivation which made all these things possible. To my family members and friends who are present in my life, for their encouragement and love given to me.

ACKNOWLEDGEMENTS

I would like to thank my advisor, Dr. Bing Guo. He gave me not only the chance to study under his guidance but also academic advice for my research. I sincerely thank my committee, Dr. Manuel P. Soriaga and Dr. Xinghang Zhang, for their time and recommendations.

I also would like to thank my group members, who have given great help to me, Gagan Singh and Wonjoong Hwang. I appreciate Kyle Cummins for doing the XPS analysis and Dr. Maria King, for providing me various instruments in the Aerosol Technology Lab.

TABLE OF CONTENTS

Page

LIST OF FIGURES

FIGURE Page

FIGURE Page

LIST OF TABLES

1. INTRODUCTION

Carbon nanomaterials are generated as natural or anthropogenic products, and may be emitted to the environment or the work place. After generation, carbon nanomaterials may experience environmental or engineering processes such as heating or aging.

The toxicity of the carbon nanomaterials have been studied in various ways [1-5]. One of the studies shows that carbon nanomaterials can generate reactive oxygen species(ROS) by donating electrons in the presence of transition metals including iron ions. Reactive oxygen species(ROS) such as superoxide(O_2^-) and hydroxyl radical($OH^\cdot$) can bring about toxic effects on the human body by causing oxidative stress [1, 2, 6]. Specifically, the toxicity of carbon nanomaterials has been associated with the reductive capacity towards Fe^{3+} ions(RCFI) of carbon nanomaterials [4].

Even though plenty of toxicology studies have gone forward, little is known about the effects of engineering and environmental processes such as heating and exposing to various gases, on the toxicity of carbon nanomaterials. The motivation of this study was to find how engineering or environmental treatments might affect the toxicity of carbon nanomaterials.

In previous studies, surface functional group quantity changes after aging and heating treatments had been revealed [7-12]. In most cases, the oxygen-containing

---

This thesis follows the style of *Environmental Toxicology and Chemistry.*

surface functional groups were increased after aging, and the oxygen-containing surface functional groups were decreased after heating [7-9]. Aging treatment induced depletion of C-O single bond and growth of C=O double bonds(Carbonyl) [7]. Heating led to decrease of OH groups(Hydroxyl)[10]. On the other hand, surface reductive capacity of carbon nanomaterials had been related to surface functional groups. Therefore, the oxygen-containing surface functional group changes after engineering treatments would also affect on the toxicity of carbon nanomaterials by altering the surface redox capability. However, the effects of these processes on the RCFI of carbon nanomaterials have not been investigated until this study.

In previous studies, a relatively long period of time(2 months to 24 months) was needed to obtain the aging results [8]. In these studies, relatively thick layers of nanomaterials were exposed to static air. The time scale for gas diffusion through the nanomaterial layers was quantified. The long time required could be due to the long time scale of diffusion. There is a need to investigate the aging effects for shorter, environmentally relevant lengths of time.

The objective of this study was to find the pattern of RCFI changes after various heating and aging treatments and the reason of the RCFI changes. The reason of the RCFI changes was studied by examining other studies and the relation with the surface functional group changes obtained by XPS. In this way, this study would reveal how various engineering and environmental processes significantly affect on the toxicity of carbon nanomaterials.

2. MATERIALS AND METHODS

Commercially available carbon nanomaterials were purchased, and used for the various treatments. After treatments, RCFI of carbon nanomaterials was measured, and XPS analysis was carried out.

2.1 Materials and Experiment Matrix

Table 1 shows detailed information of the carbon nanomaterials that were used in this study. All the materials were purchased from commercial companies except soot-A. Soot-A particles were generated in the lab by using acetylene [13].

Table 1. Sample information of the carbon nanomaterials

Sample ID.	Materials	Physical dimensions[a]	ID # (CAS/Lot)	Manufacturer
CB	Carbon Black (Printex 90)	Mean diameter : 14 nm	C1333-86-4	Degussa
Soot-A	Soot generated from acetylene	Mean diameter : 52.8 nm [14]	N/A	In-house
SCNT_1	Single-wall carbon nanotubes	Outer Diameter : 1-2 nm Length : 5-30 μm	Sku-0101	Cheap Tubes
SCNT_2	Single-wall carbon nanotubes with OH groups	Outer Diameter : 1-2 nm Length : 10-30 μm	Sku-0102	
SCNT_3	Single-wall carbon nanotubes with COOH groups	Outer Diameter : 1-2 nm Length : 5-30 μm	Sku-0103	
MCNT_1	Multi-wall carbon nanotubes	Outer Diameter : < 8 nm Length : 10-30 μm	Sku-030101	
MCNT_2		Outer Diameter : 10-20 nm Length : 10-30 μm	Sku-030103	
MCNT_3		Outer Diameter : > 50 nm Length : 10-20 μm	Sku-030107	
MCNT_4	Graphitized MCNT_2	Outer Diameter : 10-20 nm Length : 10-30 μm	Sku-030103	
MCNT_5	Graphitized MCNT_3	Outer Diameter : > 50 nm Length : 10-20 μm	Sku-030107	

Table 1 continued

Sample ID.	Materials	Physical dimensions[a]	ID # (CAS/Lot)	Manufacturer
GNP_1	Graphene Nano Platelets Grade 1	Diameter : 5 µm Average Thickness : 15 nm	N/A	Cheap Tubes
GNP_2	Graphene Nano Platelets Grade 2	Diameter : 5 µm Average Thickness : 10 nm	N/A	
GNP_3	Graphene Nano Platelets Grade 3	Diameter : 2 µm Average Thickness : Sub micron	N/A	
C_{60}	Refined Mixed Fullerenes	Theoretical outer diameter : 1 nm	C99685 -96-8	MER
DPM	Diesel Particulate Matter	Mean diameter : 1.62 µm	2975	NIST
UPM	Urban Particulate Matter	200 nm – 100 µm (Mode : 20 µm)	1648a	

[*] The physical dimensions of CB, CNTs, GNPs and SRMs were provided by the manufacturers, and a theoretical value was used for C_{60}.

Table 2 shows the specific surface area for some of the carbon nanomaterials that were used in this study. The BET surface areas of SCNTs and MCNTs were obtained from Hwang's thesis [15]. The BET surface areas of carbon black and DPM were adopted from Drake's thesis[13]. The specific surface area of GNPs was provided by the manufacturer (Cheap Tubes Inc.).

Table 2. Carbon nanomaterials surface area

Sample ID.	Surface Area(m^2/g)
CB	354.5
SCNT_1	425.4236
SCNT_2 (SCNT_OH)	336.4877
MCNT_2	153.8514
GNP_1	50
GNP_2	100
GNP_3	600-750
DPM	118.7

* Surface area of CB, SCNT_1, SCNT_2, MCNT_2, and DPM was determined by BET measurements. Specific surface area of GNPs was provided by the manufacturer (Cheap Tubes Inc.).

The heating and aging treatments carried out on various carbon nanomaterials are listed in Table 3. The experimental nomenclature of this study was determined as described in Table 3.

Table 3. Experiment matrix

Carbon Nanomaterials	**RCFI**	**XPS**	**Other**
CB	**P, HH, HN, HA(0.5~5), HNM(0.5~5), HAM(0.5~5), HNC, HNCM, AA, AAM, AN, ANM, AO, AOM, ACA, ACAM, AWO, AWN, AAC, ACM**	**P, HAM, AAM, AWO**	**BET**
Soot-A	**P, HH, HN, HA, AAM, AWO**		
SCNT_1	**P, HA, AWO**		**BET**
SCNT_2	**P, HA, AWO**		**BET**
SCNT_3	**P, HA, AWO, AAM**		
MCNT_1	**P, HA, AWO, AAM**		
MCNT_2	**P, HA, AWO, AAM**		**BET**
MCNT_3	**P, HA, AWO, AAM**		
MCNT_4	**P, HA, AWO, AAM**		
MCNT_5	**P, HA, AWO, AAM**		
GNP_1	**P, HA, AWO, AAM, AWA, AWC**	**P, HA, AAM**	
GNP_2	**P, HA, AWO, AAM, AWA, AWC**	**P, HA, AWO, AAM**	
GNP_3	**P, HA, AWO, AAM, AWA, AWC, AC**	**P, HA, AWO, AAM**	
C60	**P, HA**		
DPM	**P, HA(1~3), AWO, AAM**		**BET**
UPM	**P, HA, AWO, AAM**		

* HA(Heated in air), HH(Heated in H_2/N_2), HN(Heated in N_2), HNC(Heated in N_2/CO_2), HXM(Heated in X gas with moisture), HX(a~b)(Heated in X gas at a × 100~b × 100ºC), AAM(Weathered in moist synthetic air), AA(Weathered in synthetic air), AOM(Weathered in O_2 with moisture), AO(Weathered in O_2), ANM(Weathered in N_2 with moisture), AN(Weathered in N_2), ACM(Weathered in moist synthetic air and CO_2), AAC(Weathered in synthetic air and CO_2), ACA(Weathered in air), ACAM(Weathered in moist air), AC(Weathered in CO_2), AWO(Soaked in water under O_2), AWN(Soaked in water under N_2), AWA(Soaked in water under N_2/O_2), AWC(Soaked in water under N_2/O_2 and CO_2)

2.2 Measurement of Reductive Capacity towards Fe^{3+} Ions (RCFI)

The RCFI was measured using a spectrophotometric method after incubating the carbon nanomaterial in a Fe^{3+} solution. Details are given below.

Samples were prepared for each RCFI measurement. Three replicate samples were made by using 200-ml beakers by adding 9.0 ± 0.2 mg of the Iron(III) sulfate hydrate ($Fe_2(SO_4)_3 \cdot xH_2O$, Reagent grade, Alfa Aesar, Ward Hill, MA) and 30 ± 0.2 mg of the carbon nanomaterials. In case of hydrophobic carbon nanomaterials (C60), 2 ml of 0.12 mM surfactant (Tween 20, Bio-Rad, Hercules, CA) was added. After adding 75ml of DI water each beaker, the beakers were sealed with Parafilm® (Pechiney Plastic Packing, Chicago, IL). A 10 L analog water bath (Cole Parmer, Vernon Hills, IL) was warmed up and set at 37 ˚C. The three sample solutions stayed in the water bath for 16 hours. After 16 hours of incubation, solutions were filtered into 100ml volumetric flasks through 9 cm diameter paper filters (grade 415, 28320-041, VWR, West Chaser, PA). After separating each particle-free solution, three 25-mL of particle-free solution was taken and put into three 100 ml volumetric flasks. And then, these three flasks were labeled A, B and C. 0.25 ml of 20 % of sulfuric acid (H_2SO_4, 95 %, Labchem, Pittsburgh, PA) was added to all the A, B and C flasks by using micropipettes with ranges of 40 ~ 200 µl and 200 ~ 1000 µl (Cole Parmer, Vernon Hills, IL). 1 ml of 1 % hydroquinone ($C_6H_4(OH)_2$, 99 %, Alfa Aesar, Ward Hill, MA) was added only to 'B' flask to reduce Fe^{3+} remaining in 'B' flask to Fe^{2+}. 10ml of 0.3% 1,10-phenanthroline ($C_{12}H_8N_2$, >99 %, Alfa Aesar, Ward Hill, MA) was added to 'B' and 'C' flasks for color development. 5, 10 and 25 ml of polystyrene pipettes (Becton Dickinson Labware, Franklin Lakes, NJ) were used for adding chemical compounds. Each solution was diluted to 100 ml with DI water. After leaving the solutions for 1 hour to develop their color, 2~3 ml of solution was moved to the 4.5 ml optical polystyrene cuvette (58017-880, VWR, West Chaser, PA) to measure the absorbance at wavelength 512 nm with a single-beam 1100 series Spectrophotometer (Cole Parmer, Vernon Hills, IL). Absorbance of DI water was set to zero before measurement. An ultrasonic cleaner (Model T50, VWR, West Chaser, PA) was used for cleaning glassware before and after RCFI measurements.

After the absorbance measurement, the difference between absorbance of Fe^{2+}(Flask 'C') and absorbance of method blank (Flask 'A') was calculated. The difference indicates intensity of color due to purely Fe^{2+}. The corresponding Fe^{2+} ions concentration (mg/L) in the solution could be found by multiplying the slope of the calibration curve to the absorbance difference between flask A and C. The detailed RCFI calculation is described in Appendix B.

Transition iron (Fe^{3+}) was incubated without carbon nanomaterials by adding 9.0 ± 0.2 mg of the Iron(III) sulfate hydrate in 200-ml beakers with 75ml of DI water to measure the original Fe^{2+} concentration. Three replicate samples were made and incubated in the water bath for 16 hours. After 16 hours of incubation, RCFI of transition iron was measured as the same procedure above. The RCFI of transition iron without carbon nanomaterials was 8.22×10^{-4}g/g. This indicates that the Iron(III) sulfate hydrate originally contains a small amount of Fe^{2+} in itself.

2.3 Treatment Methods and Variables

2.3.1 Atmosphere Settings in Heating Treatments

Various heating apparatuses were installed so that different heating atmospheres could be used. For each heating treatment, a total of 110mg carbon nanomaterial was placed in an alumina crucible and heated in a tube furnace.

Fig. 1 (a) is a schematic of the heating treatment under various atmospheres. Gas tubes were connected to the furnace tube. For 5mol% H_2 and 95mol% N_2 atmospheres, N_2 gas was flown thorough the furnace at 1 standard liter per minute(SLM) for 2 minutes; then H_2 gas was turned on at 50 standard cubic centimeter per minute(sccm) so that 5% H_2 gas flow rate could be obtained. The furnace was heated up to 200˚C at a temperature ramping rate of 5 ºC/min, and maintained at the maximum temperature for 2 hours. After 2 hours at 200˚C, the heating element was turned off, and the H_2/N_2 flow rates kept unchanged. Once the temperature decreased below 50˚C, the gases were turned off, and the particles were retrieved.

After the heating treatments, 90mg of the carbon nanomaterial was used for the RCFI measurement, and 20mg was used for the XPS measurement if applicable.

Heating treatment was carried out in 100% N_2 gas atmosphere. The procedure was the same as described above except that the H_2 gas tube was retracted and only N_2 gas was flown into the furnace at 1 SLM.

Heating treatment in the air was carried out in a manner similar to what is described above after retracting the gas tubes and disconnecting both ends of the tube to open to the air.

Also, carbon black particles were heated with moist air or N_2 gas as shown in Fig. 1 (b). A gas tube was connected to the flask that contained DI water, and 1 SLM of compressed air or N_2 was flown into the flask and bubbled through the water so that the gas could flow into the quartz tube with containing the moisture.

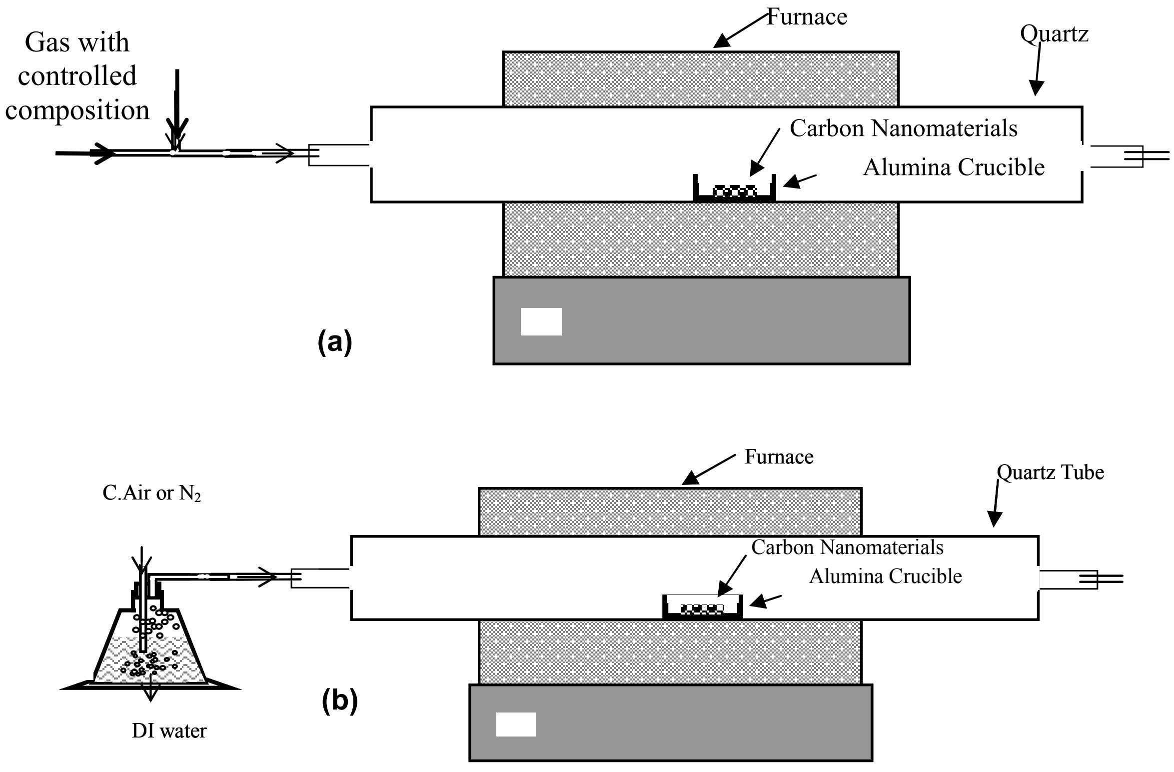

Fig. 1. Heating in various gas atmospheres. (a) Heating in various gas atmospheres without moisture (b) Heating in various temperature with moisture

Carbon black particles were also heated in N_2 and CO_2 gases with and without moisture to examine the effect of CO_2 on carbon nanomaterials heating. In the case of the heating treatment with moisture, N_2 and CO_2 gas tubes were connected to the quartz tube, and a flask with DI water was connected between gas tubes and the quartz tube as shown in Fig. 2. After flowing 79sccm of N_2 and 21sccm of CO_2 gas, the furnace was heated up to 200˚C for 2 hours at a temperature ramping rate of 5 ºC/min. After heating, the RCFI was measured.

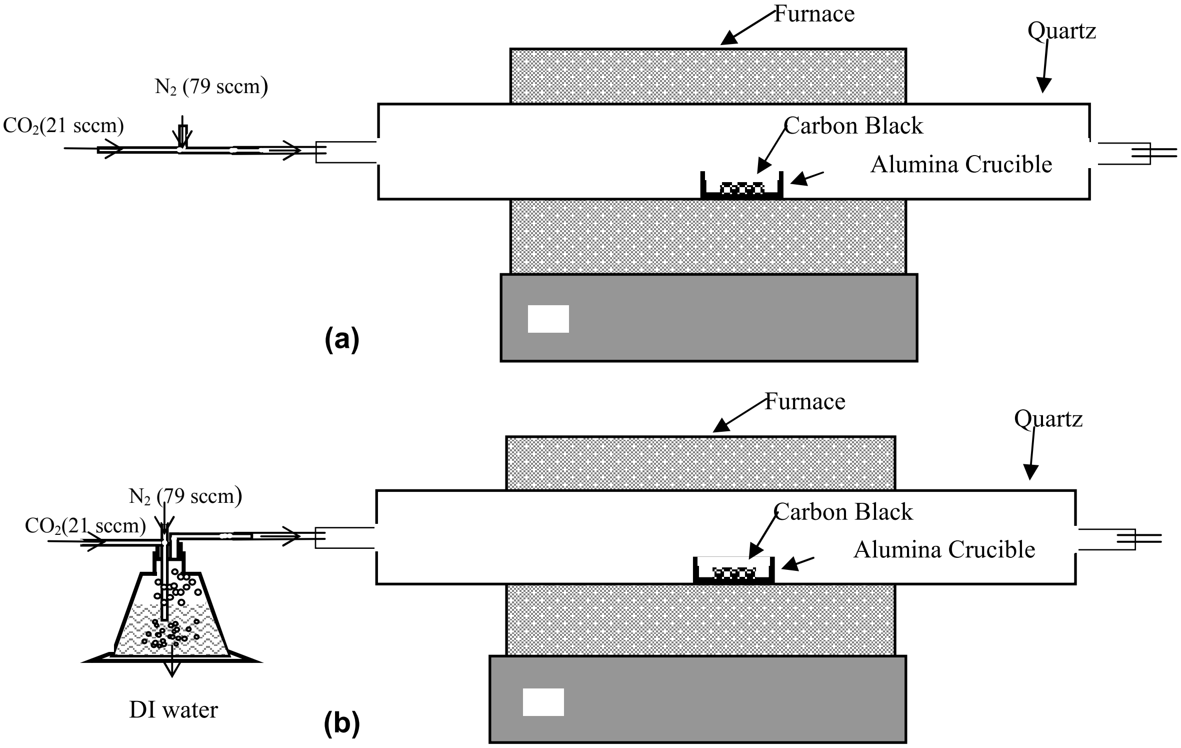

Fig. 2. Heating in N_2/CO_2. (a) Heating in N_2/CO_2 gas without moisture (b) Heating in N_2/CO_2 gas with moisture

2.3.2 Temperature Settings of Heating Treatments

Heating treatments was done in various temperature settings to examine the effects of the various heating conditions. The apparatus setup was the same as shown in Fig.1 (a).

Heating conditions were varied in the following three ways: different maximum temperatures (from 50 to 500˚C), different dwelling times at a maximum temperature of 200˚C (from 0.5 to 5 hours), and different temperature ramping rates at a 200˚C maximum temperature and a 2 hour dwelling time (from 1 to 30˚C/min). All the other values except the variable value were fixed as shown in Table 4.

Also, RCFI of carbon black particles was measured with various waiting times (from 0 to 20 hours) after completion of heating, by leaving the heat-treated carbon black particles in ambient air at room temperature. Table 4 shows the various heating conditions and the waiting times.

Table 4. Various heating conditions and waiting times

Variable Value	Numerical Value							Fixed Value
Maxumum Temperature(ºC)	50	100	200	300	400	500	·	Dwelling time 2hours, Ramping rate 5 ºC/min, Waiting time 0
Dwelling time (hours)	0.5	1	2	3	4	5	·	Maximum temperature 200ºC, Ramping rate 5 ºC/min, Waiting time 0
Temperature ramping rate(ºC/min)	1	3	5	10	15	20	30	Maximum temperature 200ºC, Dwelling time 2hours, Waiting time 0
Waiting Time (hours)	0	10	20	·	·	·	·	Maximum temperature 200ºC, Dwelling time 2hours, Ramping rate 5 ºC/min

2.3.3 Soaking in Water under Various Atmospheres

Carbon nanomaterials were soaked in water under various atmospheres as shown in Fig. 3. 120mg of carbon nanomaterials were used for the treatment by stirring in 100ml of DI(De-ionized) water for 2 weeks at 20±3˚C. As shown in the Table 5, O_2 and N_2 gas was introduced separately at 30 sccm(standard cc per minute) to compare O_2 and N_2 gas effect on oxidation(condition 1, 2), and synthetic air (N_2/O_2) and CO_2 gases were flown into the flask under two conditions(condition 3, 4) to compare N_2/O_2 and CO_2 gas effect. After 2 weeks of soaking, the RCFI measurement was done by dividing 75ml of suspension into three-25ml portions, resulting in three replicate samples. The last 25ml of suspension was used for XPS measurement.

Table 5. Various gas flow rate in soaking

Gas	Condition 1	Condition 2	Condition 3	Condition 4
N_2(sccm)	0	30	79	79
O_2(sccm)	30	0	21	21
CO_2(sccm)	0	0	0	0.5

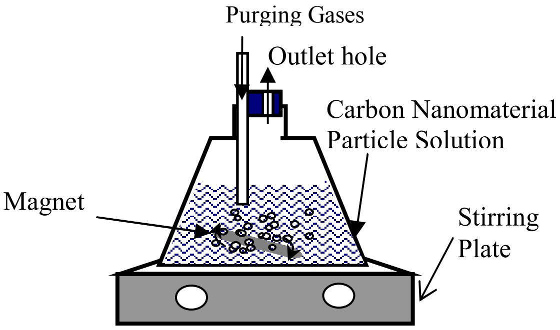

Fig. 3. Soaking in water under various atmospheres

2.3.4 Weathering in Packed Bed in Gas Flow

Carbon nanomaterials in the dry powder form were placed between two paper filters and subjected to gas flows with controlled atmospheres. As shown in Fig. 4, 110mg of carbon nanomaterial particles was spread uniformly on a 47mm filter paper and covered by another 47mm filter, to make a "sandwich". The sandwich sample was securely held in a filter holder.

The N_2/O_2 and compressed air (C.Air) gas tubes were connected to the HEPA filter (high efficiency particulate air filter). And the HEPA filter was connected to two filter holders; one filter holder was connected to the flask with DI water so that the gases can carry the moisture, and the other filter holder was connected to the HEPA filter directly. The N_2/O_2 and compressed air (C.Air) gas flow rate was controlled in four conditions in Table 6 to determine the various gas effects on weathering.

Table 6. Various gas flow rates

Gas	Condition 1	Condition 2	Condition 3	Condition 4
N_2(sccm)	100	79	0	0
O_2(sccm)	0	21	100	0
Compressed Air(sccm)	0	0	0	100

The humidity of the filter holder connected to the water flask was measured by the humidity meter (HOBO U10, 2006 Onset Computer Corporation) in front of the filter holder outlet (Humidity was 90 ± 4 %). After a week of weathering at 20±3˚C, 90mg of carbon nanomaterial sample was used for the RCFI measurement, and 20mg of carbon nanomaterial sample was used for the XPS measurement. Especially, carbon black particles were weathered in moist synthetic air for various weathering times (1, 3, 5, 7days) to determine the RCFI change in various weathering time differences. The weight change of sandwich samples was also measured after weathering to determine the mass of absorbed water.

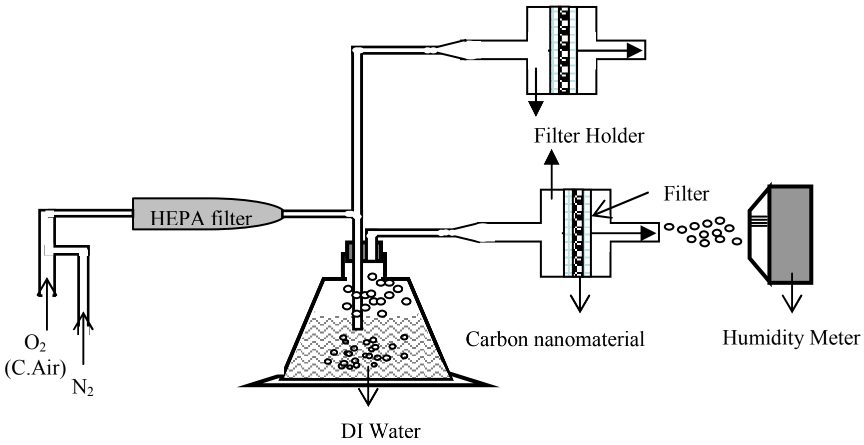

Fig. 4. Weathering in packed bed in gas flow

Carbon black was also weathered in the packed bed in synthetic air (N_2/O_2) and CO_2 gas flow to find the effect of CO_2 on weathering in synthetic air as shown in Fig. 5. The experimental procedure was the same as above except that the synthetic air and CO_2 gas tubes were connected to the HEPA filter and the gas flow rates were controlled under four conditions in Table 7 below so that 20%/10%/5%/0.5% of CO_2 gas can be flown. Other conditions such as humidity and temperature were the same as above. After a week of weathering, the RCFI of carbon black was measured by the same procedure.

Table 7. Synthetic air and CO_2 gas flow rate in weathering

Gas	Condition 1	Condition 2	Condition 3	Condition 4
N_2(sccm)	64	78	76	78.6
O_2(sccm)	16	12	19	20.9
CO_2(sccm)	20	10	5	0.5

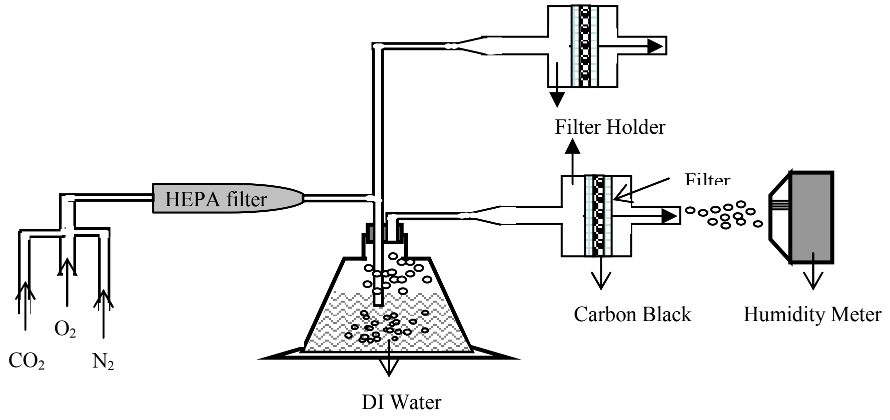

Fig. 5. Weathering in synthetic air and CO_2

2.3.5 Weathering in CO_2 for Blocking Effect

Graphene nanoplatelets grade 3 was weathered in 100% CO_2 to find the CO_2 blocking effect as shown in Fig. 6. The sandwich sample containing 180mg of GNP_3 particles was made by the same procedure above. The sandwich sample was put inside the filter holder. CO_2 gas tube was connected to the HEPA filter. 100 sccm of CO_2 gas was flown through the filter holder. After a week of weathering, CO_2 gas tube was retrieved and the sample was taken out. The RCFI of 90mg of GNP_3 was measured. The remaining 90mg of GNP_3 was put in the filter holder again. N_2/O_2 tubes were connected to the HEPA filter. And the flask with DI water was connected between the HEPA filter and the filter holder. The moist synthetic air (N_2/O_2) was flown into the filter holder. Other conditions such as humidity and temperature were the same as above. After a week of weathering, the RCFI of GNP_3 (90mg) was measured.

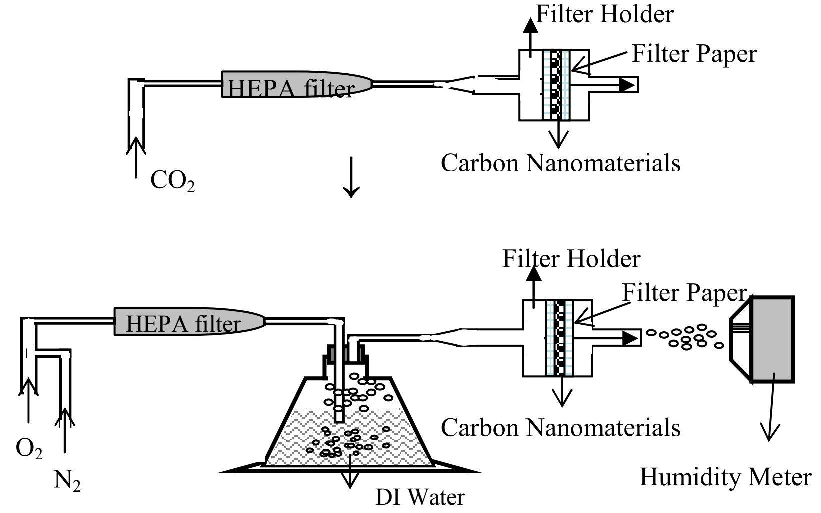

Fig. 6. Weathering in CO_2 for blocking effect

2.3.6 Weathering in Still Atmosphere

Carbon black particles were weathered in still atmosphere for various times as shown in Fig. 7. 110mg of carbon black particles were uniformly spread on the bottom of a 47mm diameter petri dish. The petri dish was placed on a plate over the water surface in the water bath. The water bath was covered, and the weathering treatments were done for various times (1, 2, 3, 4 weeks). The cap was opened for 10 minute once a day to refresh the air inside. Room temperature was kept at 20 ± 3 ˚C during the treatment. The relative humidity inside the water bath was 96 ± 2%. After weathering, the RCFI of carbon black particles was measured. The weight after weathering was also measured to determine the mass of absorbed water.

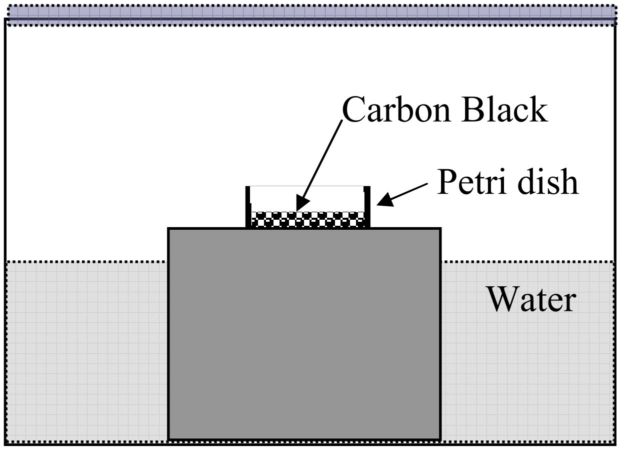

Fig. 7. Weathering in still atmosphere

2.3.7 Weathering in Grazing Gas Flow

Carbon black particles were subjected to a grazing moist air for a week as shown in Fig. 8. 110mg of carbon black particles were uniformly spread on the bottom of a 47mm diameter petri dish. The petri dish was placed on a plate over the water surface in the water bath. The water bath was covered, and the left side was connected with the N_2/O_2 and CO_2 tubes. The other side was connected with the outlet tube. Synthetic air (N_2/O_2) and CO_2 gases were flown into the water bath as the two flow rate conditions are shown in Table 8. Room temperature was kept at 20 ± 3 ˚C during the treatment. After weathering, the RCFI of carbon black particles was measured. The weight after weathering was also measured to determine the mass of absorbed water.

Table 8. Grazing gas flow rate

Gas	Condition 1	Condition 2
N_2(sccm)	79	79
O_2(sccm)	21	21
CO_2(sccm)	0	0.5

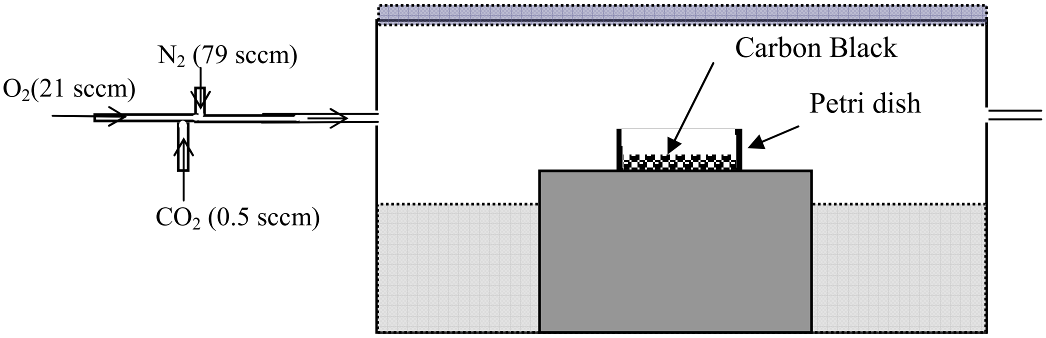

Fig. 8. Weathering in grazing gas flow

2.3.8 Weathering in Still Air and Various Lighting Conditions

Several samples were prepared by spreading 110mg of carbon black particles on a 47mm filter paper uniformly. One sample was wrapped with aluminum foil so that the carbon black particles would remain in darkness, and the other sample was not wrapped so that the carbon black particles would be exposed to the room light and the natural daylight. The two samples were placed in separate petri dishes, and the cap was covered so that there would not be any direct contaminations. Three replicate samples were made in the same way as shown in Fig. 9. The petri dishes with the samples were left on the shelf. The RCFI of each samples were measured after 1, 2 and 3 months.

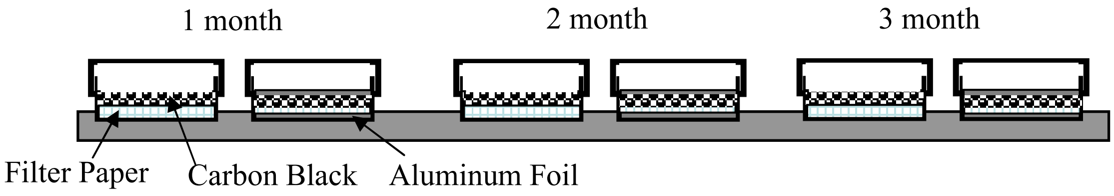

Fig. 9. Weathering in still air and various lighting conditions

2.3.9 Treatment Cocktails

Carbon black samples were subjected to combined treatments. Carbon black particles were heated at 200ºC for 2 hours in air and soaked or weathered. 120mg of heat-treated carbon black particles were soaked for two weeks in water under O_2as shown in Fig. 3. 110mg of heat-treated carbon black particles were weathered for a week in moist synthetic air (N_2/O_2) as shown in Fig. 4. After soaking or weathering, the RCFI of heat-treated carbon black was measured.

2.3.10 Diffusion Time Calculation for Weathering Treatments

Before weathering treatments in air were carried out, diffusion time was needed to be calculated. To determine the weathering time, the diffusion coefficient should be considered and calculated. After setting up the weathering apparatus shown in Fig. 4, the diffusion coefficient was calculated by considering the air diffusion to the packed carbon black particles in the filter.

According to STANLEY-WOOD et al., Knudsen Diffusion Coefficient ($D\kappa$) is defined as[16];

$$D\kappa = \frac{4r}{3}\left(\frac{2RT}{\pi M}\right)^{\frac{1}{2}}\left(\frac{(1-f)}{2}\right) \tag{1}$$

R is gas constant, M is molecular weight. r is radius of a capillary or an equivalent void through a packed powder. f is proportion of the molecules striking the surface [16].

Knudsen had used the very small value of f, which is equal to 0.98. $\left(\frac{2RT}{\pi M}\right)^{\frac{1}{2}}$ in air was calculated in STANLEY-WOOD et al. Accordingly, equation (1) can be defined as [16];

$$D\kappa = \frac{4r}{3}(2.325cm/s)\left(\frac{(1-0.98)}{2}\right) \tag{2}$$

This equation was used to calculate the diffusion time for weathering by determining radius of an equivalent void (r) in carbon black particles. And the detailed calculation is described in the results.

2.4 XPS Analysis

X-ray photoelectron spectroscopy (XPS) was carried out for some samples of carbon nanomaterials after treatments. The Kratos Axis Ultra Imaging XPS (Kratos Analytical, Manchester, UK) was used for the XPS analysis of surface functional group changes after treatments. The following are typical settings for XPS data acquisition: Analyzer Mode – Spectrum; Lens mode – Hybrid; Resolution – Pass energy 160; Aperture – Slot; Anode– Mono(Al); Current (mA) – (10); Anode HT (kV) – (12); Charge Neutralizer – on for acquisition; Type- spectrum; B.E.; Ref. – Mono(Al); Energy regions – On. In scan control section, proper scan parameters were typed. The following are typical settings for survey scan; Center eV: (700) ; Width eV: (1400); Step eV: (0.5); Sweeps: (300); #Sweeps: (3). The following are typical settings for high resolution scan; Width eV (2~3 eV higher than the default setup); Step eV : (0.1 eV); Sweeps : (60s); #Sweeps : (>3). After XPS data acquisition, XPS deconvolution was carried out by Kyle Cummins for the quantitation of surface functional groups[17, 18]. The XPS deconvolution data was analyzed with the RCFI results.

2.5 Statistical Analysis

Analysis of variance (ANOVA) was used to determine whether the RCFI results were significantly different before and after treatments. The RCFI results were obtained from triplicate samples in each measurement to minimize possible errors. The RCFI difference within a group of more than two materials was estimated by one-way ANOVA with a significance level of 0.05 ($p = 0.05$) to see the significance of the RCFI difference before and after treatments. All the RCFI results were described as mean ± standard deviation.

3. RESULTS

The RCFI of carbon nanomaterials after various engineering treatments was determined. Heating generally led to the significant increase in RCFI, regardless of the atmosphere. Aging with O_2 resulted in significant decrease in RCFI. Water vapor enhanced the aging effect of O_2. CO_2 had a “blocking” effect, hindering the aging effect by O_2.

3.1 RCFI of Pristine Carbon Nanomaterials

As shown in Fig. 10, the RCFI of all the pristine carbon nanomaterials listed in Table 1 was measured. The RCFI of the carbon nanomaterials ranged from 0.16×10^{-3} to 34.07×10^{-3} g/g. The graphene nanoplatelets grade 3(GNP_3) had the highest RCFI, and the fullerene (C60) had the lowest RCFI. Average RCFI of carbon nanomaterials was 6.59×10^{-3}g/g.

The RCFI of pristine carbon nanomaterials was recalculated as the surface area which is described in Table 2. Table 2 and Fig 11(a) show that the RCFI is not proportional to specific surface area. In addition, if the RCFI is proportional to the specific surface area, the RCFI of carbon nanomaterials recalculated based on the specific surface area in Fig. 11 (b) would be in the same range. Accordingly, this result indicates that the RCFI is not proportional to the specific surface area. On the other hand, SCNT with hydroxyl (OH) surface groups (SCNT_2) had the higher RCFI than the pristine SCNT because the OH surface groups help the reduction of Fe^{3+} as the following reaction:

$$\sim C\text{-}OH + Fe^{3+} \rightarrow \sim C{=}O + Fe^{2+} + H^{+} \quad [19]$$

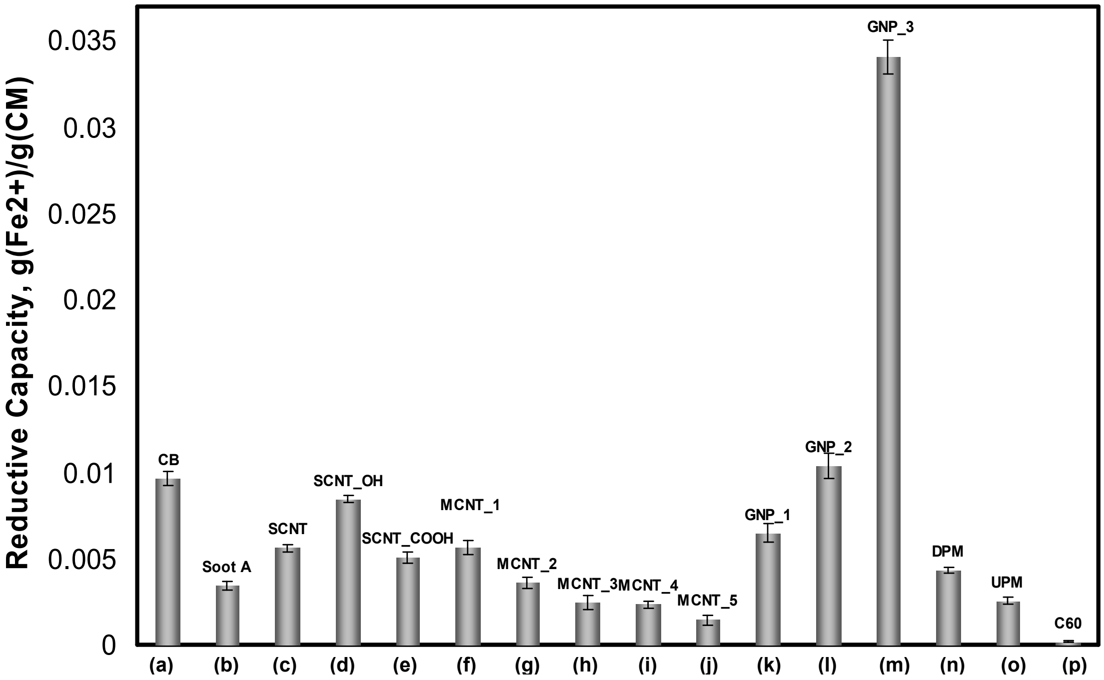

Fig. 10. RCFI of pristine carbon nanomaterials. (a) Pristine carbon black (b) Pristine soot A (c) Pristine SCNT (d) Pristine SCNT with OH groups (e) Pristine SCNT with COOH groups (f) Pristine Multi-wall CNT with outer diameter (OD) of < 8 nm (g) Pristine Multi-wall CNT with OD of 10 - 20 nm (h) Pristine Multi-wall CNT with OD of > 50 nm(MCNT_3) (i) Pristine Graphitized MCNT_2(MCNT_4) (j) Pristine Graphitized MCNT_3(MCNT_5) (k) Pristine GNPs grade 1 (l) Pristine GNPs grade 2 (m) Pristine GNPs grade 3 (n) Pristine UPM(Urban Particulate Matters) (o) Pristine DPM(Diesel Particulate Matters) (p) Pristine Fullerenes(C60)

Error bar indicates standard deviation.

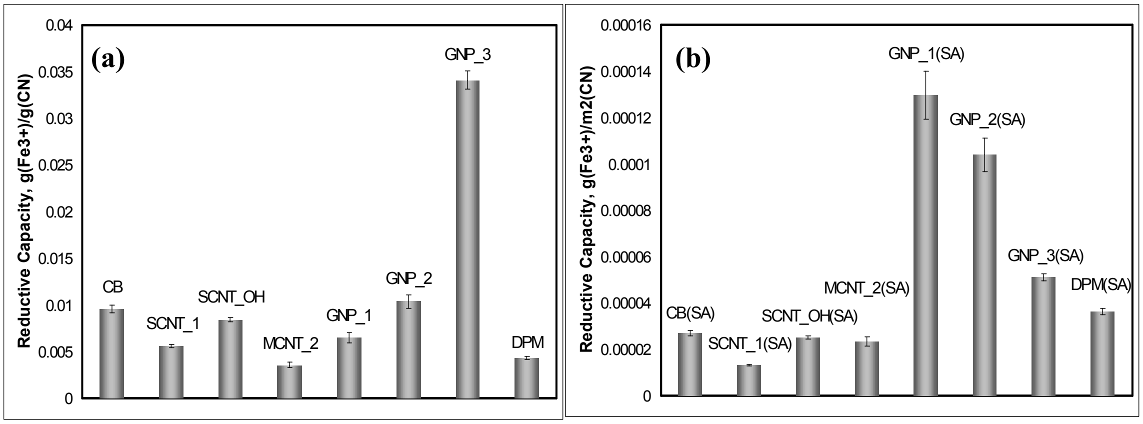

Fig. 11. RCFI of carbon nanomaterials based on surface area. (a) RCFI of pristine carbon nanomaterials (b) RCFI of carbon nanomaterials based on surface area

Error bar indicates standard deviation.

3.2 Effect of Heating

3.2.1 Heating Generally Led to Increase of RCFI

Fig. 12 shows that the RCFI of heated carbon black and soot A was significantly increased after being heated in three different gas conditions (100% N_2, 5% H_2, and air). The extent of RCFI changes in the three conditions was similar. This result shows that heating treatments induce significant increase in RCFI, regardless of the atmosphere under which the carbon nanomaterials were heated. The RCFI of carbon black was increased from 0.96×10^{-2} to the range of $1.22\times10^{-2} \sim 1.28\times10^{-2}$ g/g. The RCFI of soot A was increased from 0.34×10^{-2} to the range of $0.48\times10^{-2} \sim 0.50\times10^{-2}$ g/g. This extent of RCFI change indicates that the RCFI of carbon black can be increased by 27~33%, and the RCFI of soot A can be increased by 41~47% after heating.

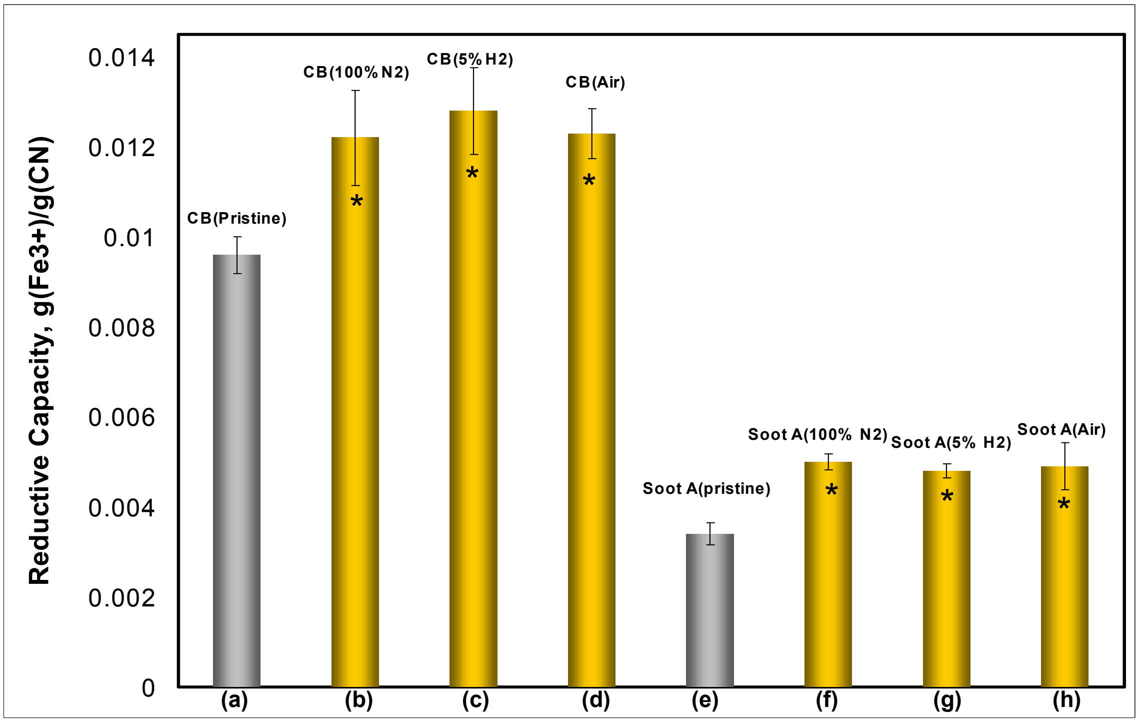

Fig. 12. RCFI of heated carbon black and soot A. (a) Pristine Carbon black (b) CB heated in 100% N_2 gas (c) CB heated in 5%H_2/95% N_2 gas (d) CB heated in air (e) Pristine Soot A (f) Soot A heated in 100% N_2 gas (g) Soot A heated in 5%H_2/95%N_2 gas (h) Soot A heated in air

'*' means significantly different from pristine sample according to the ANOVA (p: 0.05).
Error bar indicates standard deviation.

Various carbon nanomaterials were heated in air at 200ºC for 2 hours, and the significant RCFI increase was found in most cases.

Fig. 13(a) shows that the RCFI of all the three single-wall carbon nanotubes was significantly increased after heating. This result indicates that the RCFI of single-wall carbon nanotubes can be increased by 48~62% after heating.

As shown in Fig. 13(b), the RCFI of all the multi-wall carbon nanotubes was increased by 11~42% after heating. However, only the MCNT_1 and MCNT_2 had the significant difference of RCFI change after heating. This result shows that the MCNT_1 and MCNT_2 are more easily affected by the heating treatment than the other MCNTs.

The Fig. 13(c) indicates that the RCFI of graphene nanoplatelets (GNPs) grade 1 and 2 was significantly increased after heating. On the other hand, the RCFI of GNPs grade 3 was decreased after heating. GNP grade 3 was the only material whose RCFI was decreased after heating. The RCFI of GNPs grade 1 and 2 was increased by 22~24%, while the RCFI of GNPs grade 3 was decreased by 9% after heating.

Fig. 13(d) shows that the RCFI of fullerenes(C60) and SRMs(UPM, DPM) was all significantly increased after heating. The RCFI of C60 and SRMs increased 2 ~ 3 times after heating. This indicates that the RCFI of fullerenes and SRMs was strongly affected by the heating treatment.

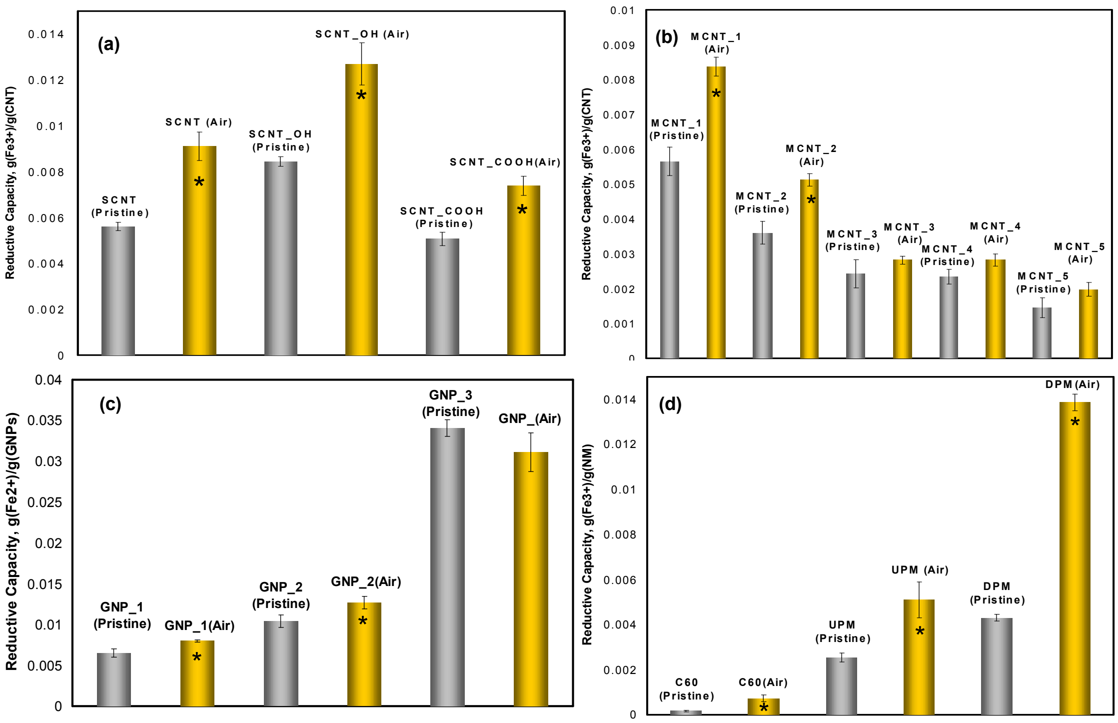

Fig. 13. RCFI of various heated carbon nanomaterials. (a) RCFI of pristine and heated single-wall CNTs (b) RCFI of pristine and heated multi-wall CNTs (c) RCFI of pristine and heated GNPs(Graphene nanoplatelets) (d) RCFI of pristine and heated fullerenes(C60) and SRMs(Standard reference materials)

'*' means significantly different from pristine sample according to the ANOVA (p: 0.05). Error bar indicates standard deviation.

3.2.2 Effects of Moisture and Temperature Settings on Heating Treatment

Carbon black was heated in compressed air with moisture and N_2 with moisture as various temperatures as shown in Fig. 1(b). Fig. 14 indicates that the RCFI increase after heating was greater when the atmosphere contained water vapor. This result shows that the water moisture enhances the RCFI increase of carbon black when it is treated with the proper heat temperature. In addition, the carbon black was not burnt when it was heated at 500ºC in N_2 gas with moisture unlike the carbon black heated at 500ºC in air with moisture and without moisture due to the lack of the oxygen.

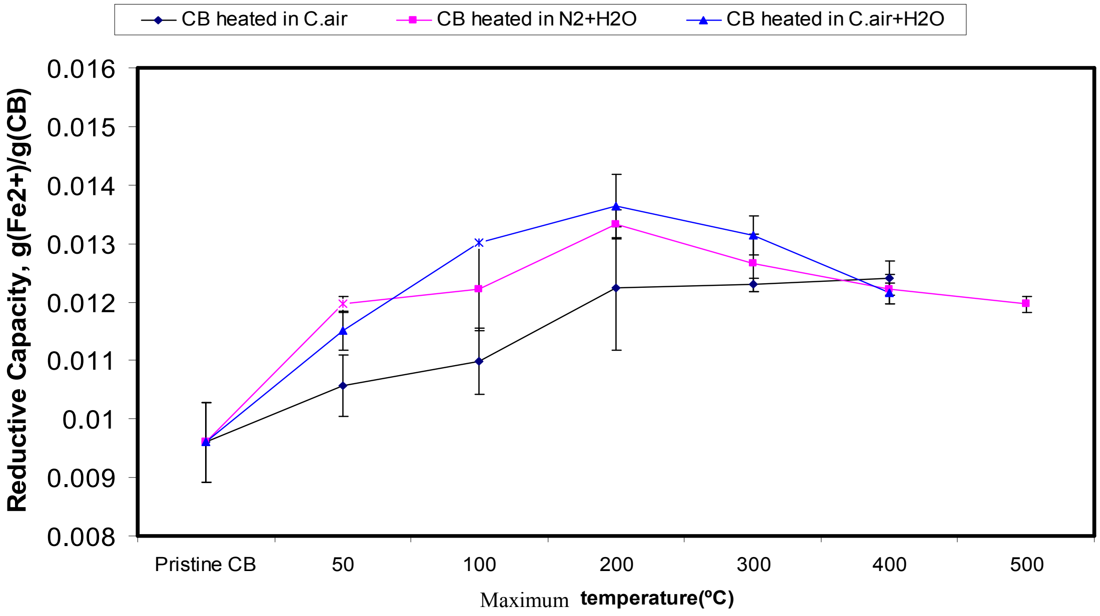

Fig. 14. RCFI of heated carbon black in various temperatures with moisture
'*' means significantly different from pristine sample according to the ANOVA (p: 0.05).
Error bar indicates standard deviation.

3.2.3 CO_2 Had No Significant Effect on Heating

The carbon black particles were heated in N_2 and CO_2 gases to determine the effect of CO_2 gas on the heating treatment as shown in Fig. 2. The result, shown in Fig. 15 indicates that the RCFI of carbon black was significantly increased after in both cases of heating in N_2 and CO_2 gases with moisture or without moisture. When it is compared to the result of heating in pure N_2, this result shows that the CO_2 gas does not affect the heating treatment. And the RCFI of carbon black heated in N_2/CO_2 increased more when it was heated with moisture. This result is the same as the result of Fig. 14 in the point that the water enhances the increase of RCFI in the heating treatment.

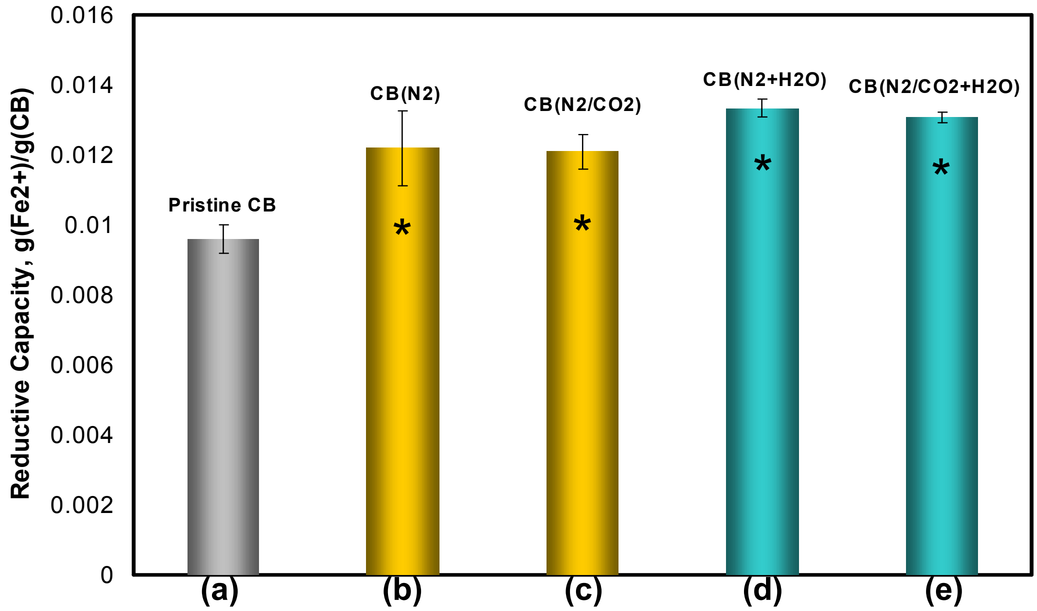

Fig. 15. RCFI of heated carbon black in N_2 and CO_2 gases. (a) pristine CB (b) CB heated 200ºC for 2 hours in N_2 (c) CB heated 200ºC for 2 hours in N_2/CO_2 (d) CB heated 200ºC for 2 hours in N_2 with moisture (e) CB Heated in N_2/CO_2 gas with moisture

'*' means significantly different from pristine sample according to the ANOVA (p: 0.05).
Error bar indicates standard deviation.

3.2.4 RCFI of Carbon Black Heated under Various Heating Conditions

Carbon black particles were heated in various conditions as shown in Table 4 to determine the effects of heating conditions on the RCFI changes. The results were shown in Fig. 16. Fig. 16 (a) indicates that the RCFI of carbon black particles increased as the temperature increased to 200ºC, but it was consistent over 200ºC. And the carbon black was burnt and lost most of its weight when it was heated at 500ºC for 2 hours in air. This result means that the carbon black particles should be heated at least at 200ºC to get the maximum RCFI increase after heating.

As shown in Fig. 16 (b), the RCFI of carbon black particles continually increased as the dwelling time increased up to 1 hour. However, it stayed consistent after 1 hour of dwelling time. This result indicates that the carbon black needs to be heated at least for 1 hour of dwelling time at 200ºC to attain the maximum RCFI increase.

Fig. 16 (c) shows that the RCFI change of carbon black was consistent until 5ºC/min of increasing ramping rate, but it was decreased when the ramping rate was increased more than 5ºC/min. This result reveals that the ramping rate of heating carbon black particles should be less than 5 ºC/min to get the maximum value of RCFI change.

As shown in Fig. 16 (d), a waiting time of up to 20 hours before RCFI measurement had no influence on the RCFI of heated carbon black particles.

According to this result of various heating conditions, heating carbon nanomaterials in air at 200ºC and 5ºC/min ramping rate for 2 hours was determined as the standard heating condition for the heating treatment of carbon nanomaterials.

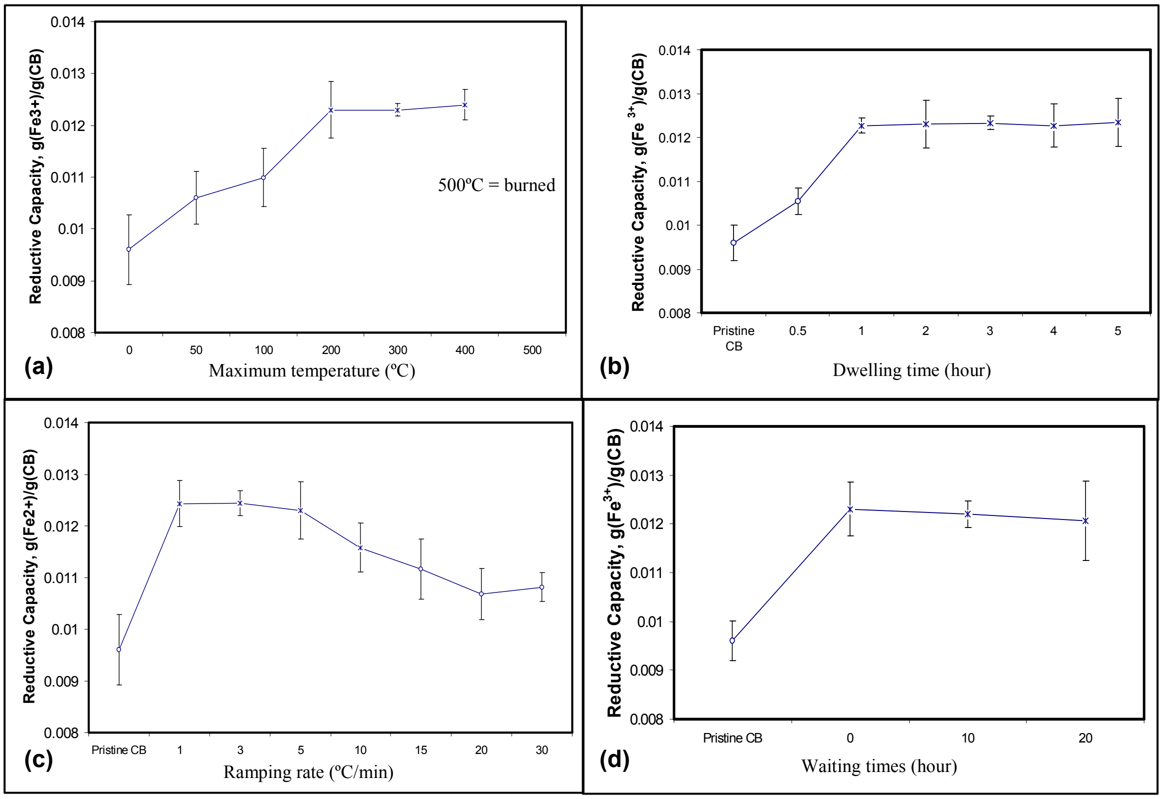

Fig. 16. RCFI of carbon black heated under various heating conditions. (a) heated in various maximum temperature (b) heated for various dwelling time (c) heated as various ramping rates (d) various waiting times after heating

'*' means significantly different from pristine sample according to the ANOVA (p: 0.05).
Error bar indicates standard deviation.

Also, the RCFI of DPMs was measured after heating at various temperatures. As shown in Fig. 17, The RCFI of DPM was increased as the maximum temperature increased. The RCFI of heated DPMs was most significantly increased between 140ºC and 200ºC, and it was consistent after 200 ºC. This result indicates that the different carbon nanomaterials can have the different aspects of RCFI increase by heating.

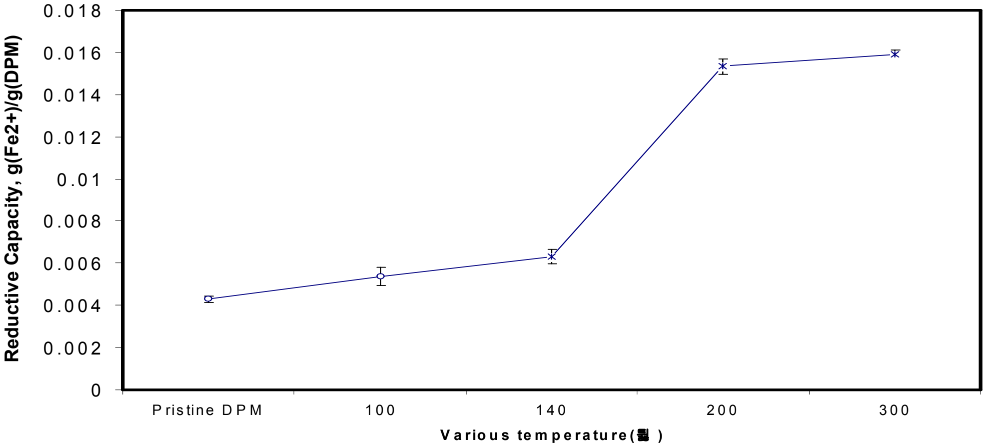

Fig. 17. RCFI of heated DPM in various temperatures

'*' means significantly different from pristine sample according to the ANOVA (p: 0.05). Error bar indicates standard deviation.

3.3 Effect of Soaking in Water

3.3.1 Soaking in Water under O_2 Led to Decrease of RCFI

Carbon black and soot A particles were soaked in water for 2 weeks under O_2 and N_2 respectively, as shown in Fig. 3. The result, shown in Fig. 18 indicates that the RCFI of carbon black and soot A was significantly decreased after soaking in water under O_2 gas. The RCFI of carbon black was decreased by 24%, and the RCFI of soot A was decreased by 16% after soaking in water under O_2. On the other hand, RCFI of carbon black was not significantly decreased after soaking in water under N_2 gas. The RCFI decrease of carbon black soaked in water under N_2 gas was 10%. This result shows that the N_2 gives no critical effect on the soaking, and the O_2 gas enhances aging of the carbon nanomaterials in water.

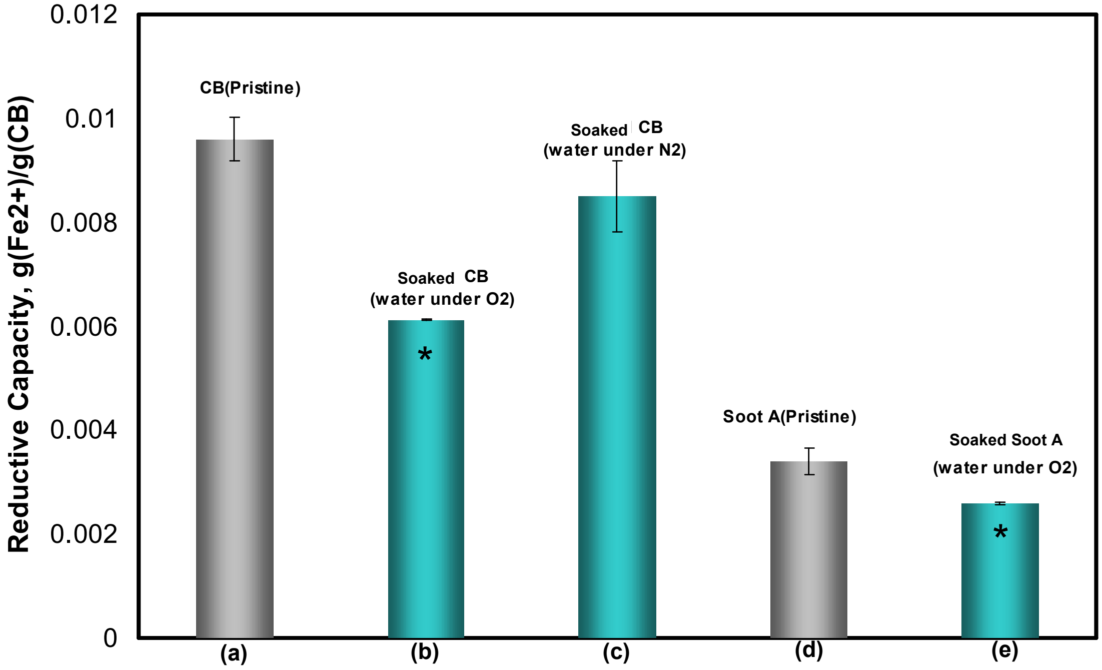

Fig. 18. RCFI of carbon black and soot A soaked in water. (a) pristine CB (b) CB soaked in water under O_2 gas (c) CB soaked in water under N_2 gas (d) pristine Soot A (e) Soot A soaked in water under O_2 gas

'*' means significantly different from pristine sample according to the ANOVA (p: 0.05). Error bar indicates standard deviation.

3.3.2 Other Carbon Nanomaterials Soaked in Water under O_2

Various carbon nanomaterials were soaked in water under O_2 for 2 weeks, and the significant RCFI decrease was found in most cases.

Fig. 19(a) shows that the RCFI of single-wall carbon nanotubes (SCNTs) was decreased after soaking in water under O_2 gas. The decrease was within the range of 15~38%. The RCFI changes of SCNTs with OH and COOH groups had significant differences. But only the RCFI change of pristine SCNTs was not significant.

As shown in Fig. 19(b), the RCFI of multi-wall carbon nanotubes (MCNTs) was decreased after soaking in water under O_2 gas. The RCFI of MCNTs was decreased by 15%~38%. Among the five MCNTs, MCNT_3 was the only material which did not experience the significant RCFI decrease.

The result in Fig. 19(c) shows that the RCFI of both standard reference materials was significantly decreased after soaking in water under O_2. The RCFI of diesel particulate matters (DPMs) was decreased by 20%, and the RCFI of urban particulate matters (UPMs) was decreased by 27% after soaking.

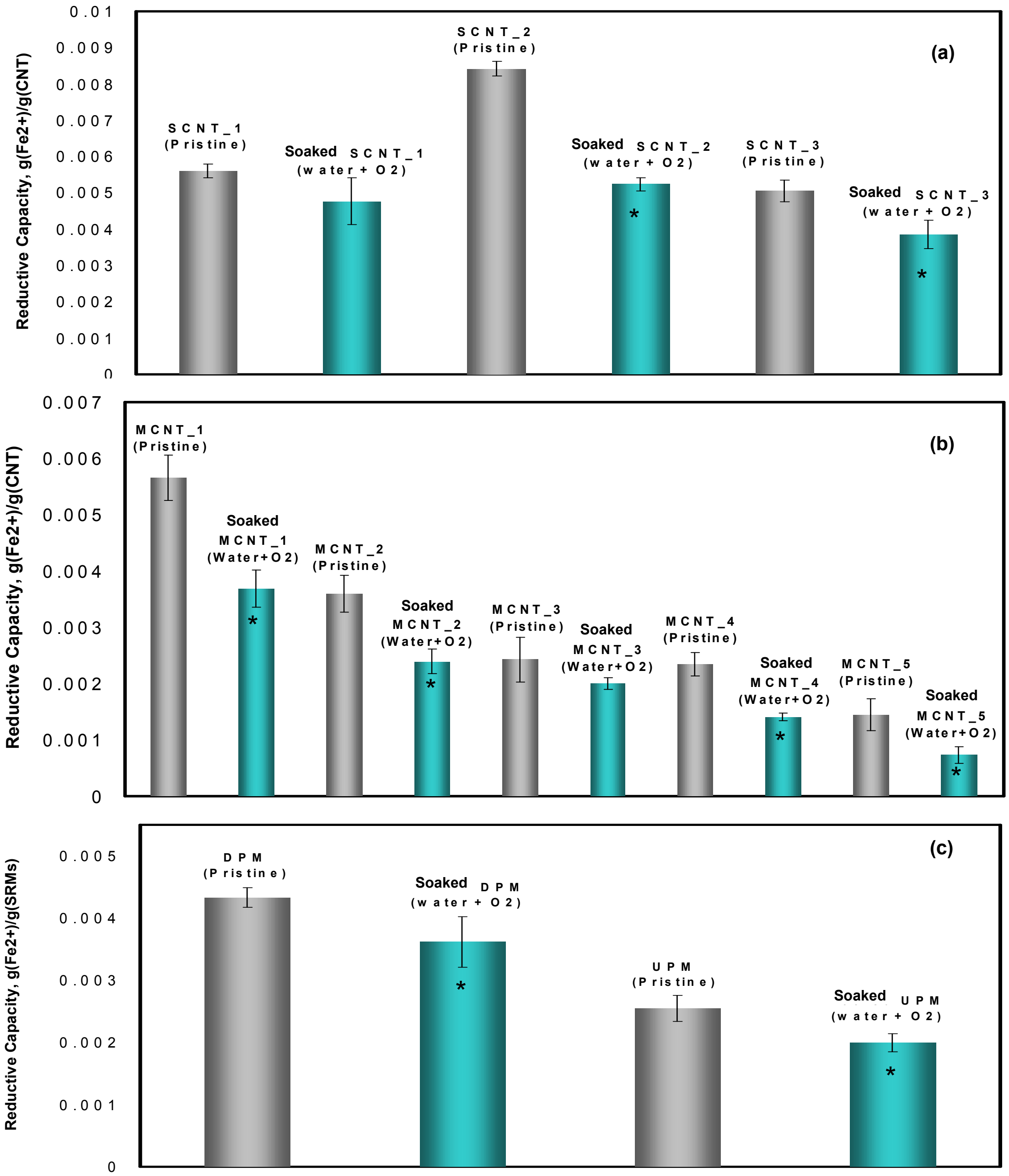

Fig. 19. RCFI of various carbon nanomaterials soaked in water under O_2. (a) RCFI of single-wall CNTs soaked in water under O_2 (b) RCFI of multi-wall CNTs soaked in water under O_2 (c) RCFI of standard reference materials (SRMs) soaked in water under O_2

'*' means significantly different from pristine sample according to the ANOVA (p: 0.05).
Error bar indicates standard deviation.

3.3.3 Graphene Nanoplatelets Soaked in Water under Various Gas Conditions

The result, shown in Fig. 20 indicates that the RCFI of graphene nanoplatelets (GNPs) was significantly decreased after soaking in water under O_2. The RCFI change of GNPs were within the range of 34~48%. Also, the RCFI of GNPs was significantly decreased after soaking in water under synthetic air (N_2/O_2). However, the RCFI decrease of GNPs after soaking in water under synthetic air was less than the RCFI decrease of GNPs soaked in water under O_2. This supports the result above that the N_2 gives no critical effect on the aging in water. In addition, the RCFI decrease after soaking in water under synthetic air and 0.5% CO_2 was less than the RCFI decrease after soaking in water under synthetic air. This result indicates that the small amount of CO_2 gas inlet may have interrupted the aging process in water suspension.

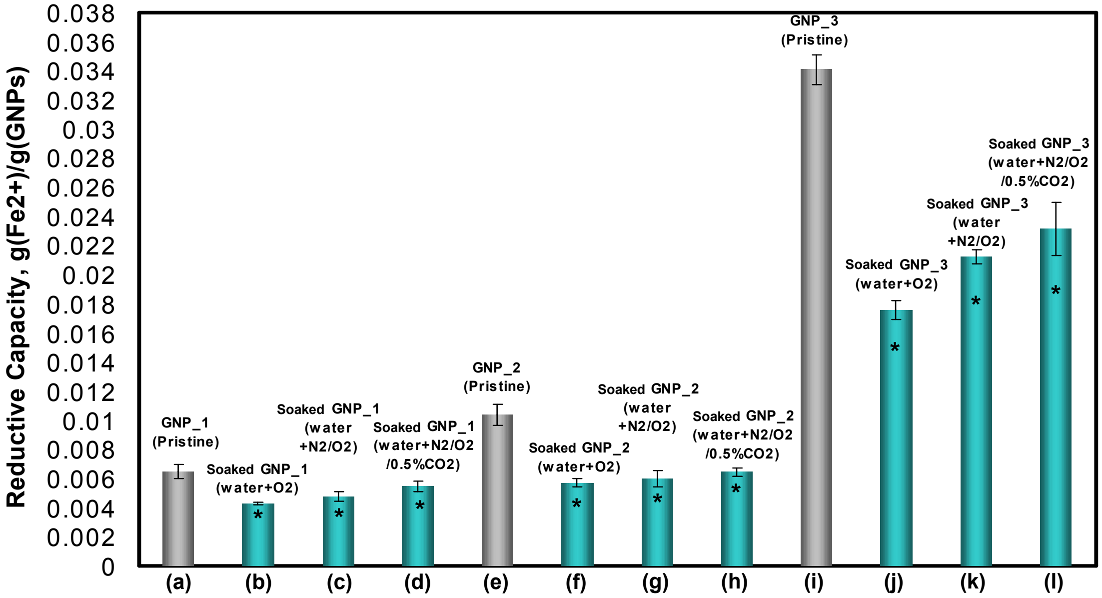

Fig. 20. RCFI of graphene nanoplatelets (GNPs) soaked in water. (a) Pristine GNP_1 (b) GNP_1 soaked in water under O_2 gas (c) GNP_1 soaked in water under synthetic air (d) GNP_1 aged in water under synthetic air/0.5%CO_2 (e) Pristine GNP_2 (f) GNP_2 soaked in water under O_2 gas (g) GNP_2 soaked in water under synthetic air (h) GNP_2 soaked in water under synthetic air/0.5%CO_2 (i) Pristine GNP_3 (j) GNP_3 soaked in water under O_2 gas (k) GNP_3 soaked in water under synthetic air (l) GNP_3 soaked in water under synthetic air/0.5%CO_2

'*' means significantly different from pristine sample according to the ANOVA (p: 0.05). Error bar indicates standard deviation.

3.4 Effect of Weathering in Gases

3.4.1 Weathering in O_2-containing Gas Led to Decrease of RCFI

Weathering of carbon black was done in packed bed with various gas flow conditions as shown in Fig. 4 and Table 6. As shown in Fig. 21, the RCFI of carbon black was decreased after weathering in various air and humidity conditions. The RCFI of carbon black was significantly decreased when it was weathered in O_2 gas (16% decrease). And the RCFI of carbon black was decreased more significantly when the carbon black was weathered in moist synthetic air (30~34% decrease). This indicates that the water moisture enhances the RCFI decrease in weathering. On the other side, the RCFI of carbon black was not decreased as much as the RCFI of carbon black weathered in moist synthetic air when the carbon black was weathered in compressed air (15% decrease). This result shows that the CO_2 in compressed air might have interrupted the aging process. Accordingly, it can be determined that both of O_2 and moisture are important factors to cause the significant RCFI decrease of weathered carbon nanomaterials, and the CO_2 can be a factor that prohibits the aging effect.

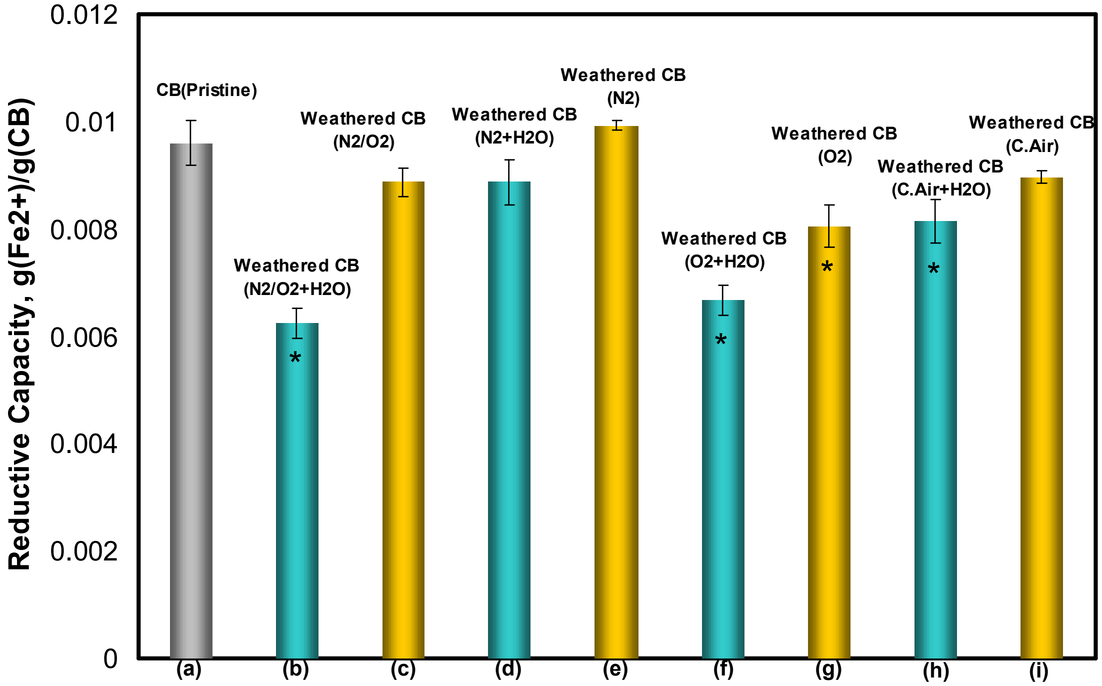

Fig. 21. RCFI of carbon black weathered in various gas conditions. (a) pristine CB (b) CB weathered in N_2 moist synthetic air (c) CB weathered in synthetic air (d) CB weathered in moist N_2 gas (e) CB weathered in N_2 gas (f) CB weathered in moist O_2 gas (g) CB weathered in O_2 gas (h) CB weathered in moist compressed air (i) CB weathered in compressed air

'*' means significantly different from pristine sample according to the ANOVA (p: 0.05).
Error bar indicates standard deviation.

Various carbon nanomaterials were also weathered in the standard weathering conditions (weathering in moist synthetic air for a week), and the significant RCFI decrease was found in most cases.

Fig. 22(a) shows that the RCFI of soot A and single-wall carbon nanotubes with COOH group (SCNT_COOH) has significantly decreased after weathering in moist synthetic air. The RCFI of Soot A was decreased by 17%, and the RCFI of SCNT_COOH was decreased by 24% after weathering.

The result, shown in Fig. 22(b) indicates that the RCFI of multi-wall carbon nanotubes (MCNTs) was decreased after weathering in moist synthetic air. The RCFI of MCNTs was decreased within the range of 10%~36%. Among five MCNTs, MCNT_5 was the only material that did not experience a significant RCFI decrease after weathering.

Fig. 22(c) indicates that the RCFI of graphene nanoplatelets (GNPs) was significantly decreased after weathering in moist synthetic air. The RCFI change of weathered GNPs were within the range of 25~44%. Most of all, the RCFI of GNP grade 1 and GNP grade 3 has decreased more than 40% percent after weathering.

Fig. 22(d) shows that the RCFI of both standard reference materials was significantly decreased after weathering in moist synthetic air. The RCFI of diesel particulate matters (DPMs) was decreased by 33%, and the RCFI of urban particulate matters (UPMs) was decreased by 28% after weathering.

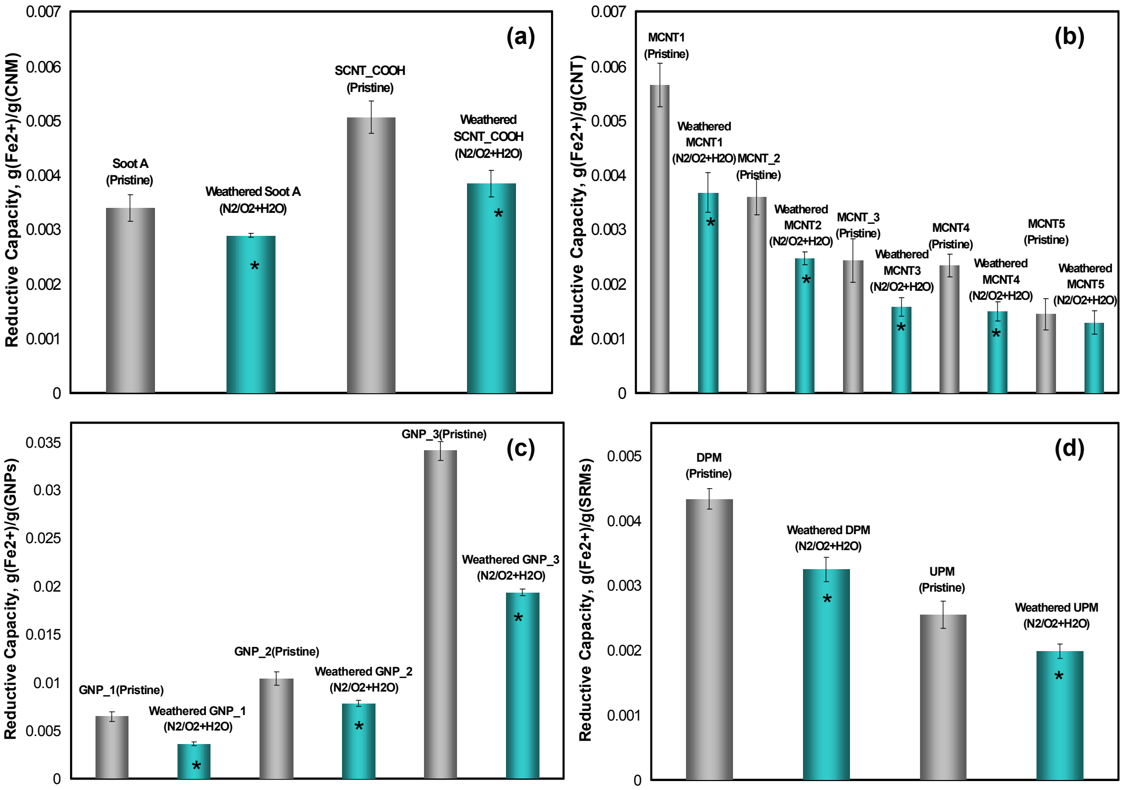

Fig. 22. RCFI of various carbon nanomaterials weathered in moist synthetic air. (a) RCFI of soot A and SCNT_COOH weathered in moist synthetic air (b) RCFI of multi-wall CNTs weathered in moist synthetic air (c) RCFI of graphene nanoplatelets (GNPs) weathered in moist synthetic air (d) RCFI of standard reference materials (SRMs) weathered in moist synthetic air

'*' means significantly different from pristine sample according to the ANOVA (p: 0.05). Error bar indicates standard deviation.

3.4.2 Weathering in Moist Synthetic Air for Various Weathering Times

The carbon black was weathered in moist synthetic air ($N_2/O_2 + H_2O$) in various weathering times. Fig. 23 shows that the RCFI of carbon black was decreased more as the weathering time increased. The RCFI difference was significant when the carbon black was weathered more than 3 days. According to the results of Fig. 22 and 23, weathering in moist synthetic air for a week was determined as the standard weathering condition for the aging in gases treatment of carbon nanomaterials.

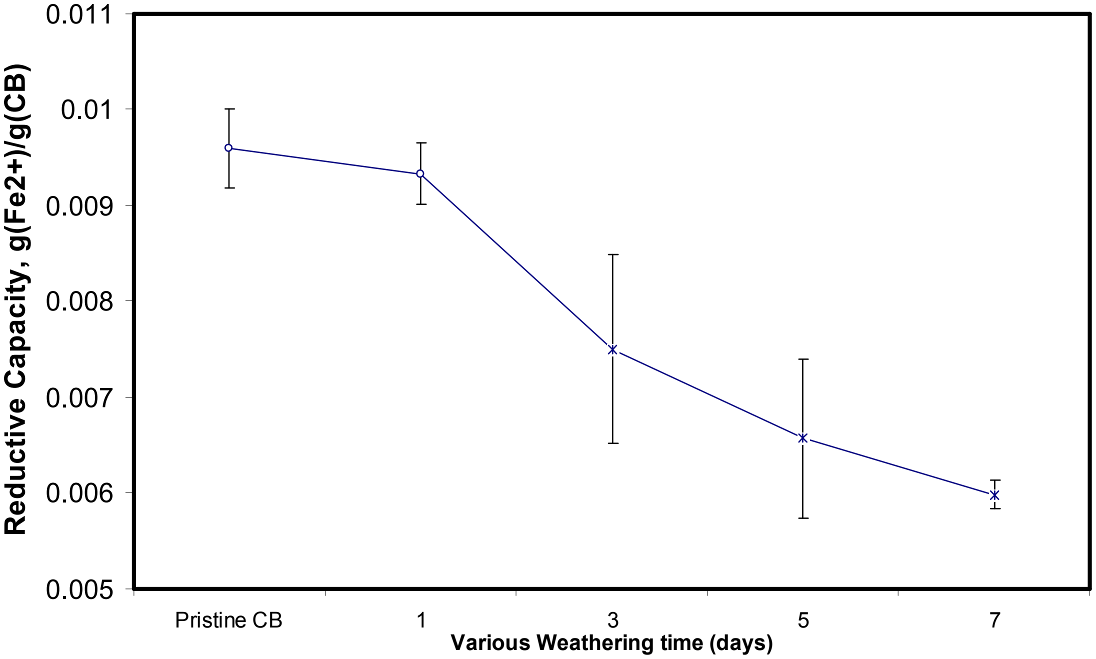

Fig. 23. RCFI of carbon black weathered in moist synthetic air for various weathering times

'*' means significantly different from pristine sample according to the ANOVA (p: 0.05).
Error bar indicates standard deviation.

3.4.3 Consideration of Absorbed Water Mass by Samples after Weathering

Water absorption during weathering in moist synthetic air was measured in order to obtain the correct mass for RCFI calculation after weathering. Table 9 shows that the mass of absorbed water after one week of weathering was only about 5% of carbon black mass. The RCFI change related to the mass of absorbed water was calculated by subtracting the water mass from the mass of the carbon black. Table 10 shows that the difference of RCFI, considering the absorbed water after one week of weathering, was 3.17×10^{-4} g/g, and it was not a significant difference. For this reason, the mass of absorbed water in sandwich samples was not considered in the RCFI of carbon nanomaterials weathered in moist synthetic air.

Table 9. Mass of water absorbed onto carbon black weathered in moist synthetic air

Time	Mass of sandwich samples before weathering (mg)	Mass of sandwich samples after weathering (mg)	Mass of absorbed water(mg)
1 day	303.5	303.7	0.2
3 days	296.7	301.0	3.3
5 days	303.4	308.5	5.1
1 week	302.4	308.4	6

* Mass of carbon black sample before weathering was 30±0.2mg

Table 10. RCFI of weathered carbon black subtracting mass of absorbed water

Time	RCFI of weathered carbon black before subtraction(g/g)	RCFI of weathered carbon black after subtraction (g/g)	RCFI differences (g/g)
1 day	9.333×10^{-3}	9.348×10^{-3}	0.15×10^{-4}
3 days	7.499×10^{-3}	7.706×10^{-3}	2.07×10^{-4}
5 days	6.569×10^{-3}	6.843×10^{-3}	2.74×10^{-4}
1 week	5.981×10^{-3}	6.298×10^{-3}	3.17×10^{-4}

3.4.4 Effect of CO_2 on RCFI Decrease in Weathering

Weathering in CO_2 containing air led to RCFI decrease less than RCFI decrease due to weathering in non-CO_2-containing air. Fig. 24 shows that the RCFI of carbon black particles was significantly decreased after weathering in moist synthetic air and CO_2. The four different CO_2 gas flow rate conditions had almost the same extent of RCFI decrease. However, the RCFI decrease after weathering in synthetic air and CO_2 was less than the RCFI decrease after weathering in synthetic air. Furthermore, the difference between the RCFI after weathering in synthetic air with CO_2 gas and the RCFI after weathering in moist synthetic air was significant. And this result was similar to the RCFI result of carbon black weathered in compressed air (C.Air). Accordingly, this fact supports the result that the small amount of CO_2 gas inlet can inhibit the effect of aging in synthetic air.

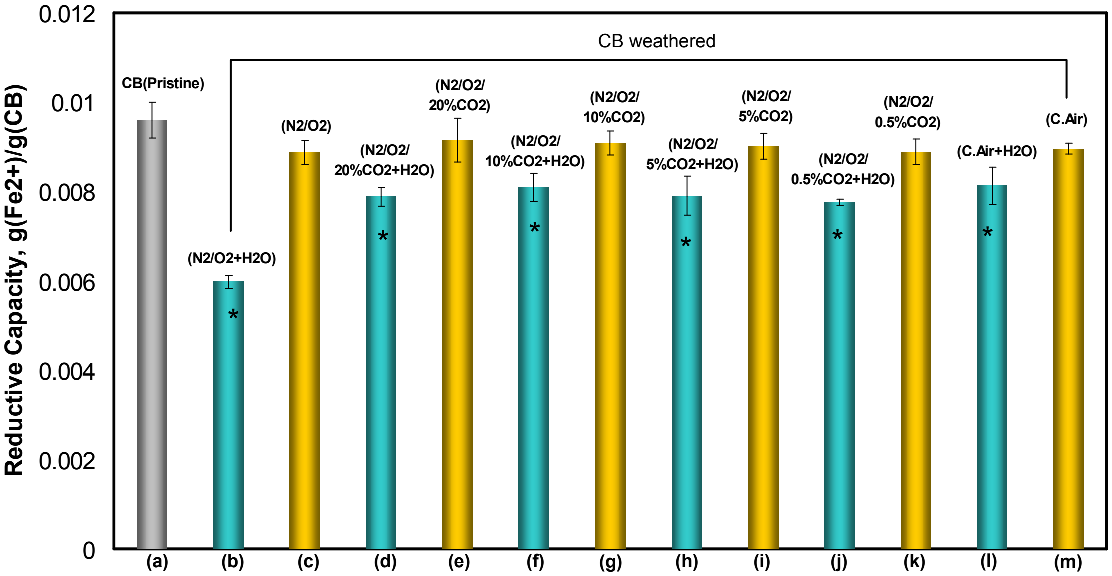

Fig. 24. RCFI of carbon black weathered in CO_2-containing air. (a) pristine CB (b) CB weathered in moist synthetic air (c) CB weathered in synthetic air (d) CB weathered in 20%CO_2/moist synthetic air (e) CB weathered in 20%CO_2/synthetic air (f) CB weathered in 10%CO_2/moist synthetic air (g) CB weathered in 10%CO_2/synthetic air (h) CB weathered in 5%CO_2/moist synthetic air (i) CB weathered in 5%CO_2/synthetic air (j) CB weathered in 0.5%CO_2/moist synthetic air (k) CB weathered in 0.5%CO_2/synthetic air (l) CB weathered in moist C. air (m) CB weathered in C. air

'*' means significantly different from pristine sample according to the ANOVA (p: 0.05).
Error bar indicates standard deviation.

3.4.5 The "Blocking" Effect of CO_2

Fig. 25 shows that the RCFI of graphene nanoplatelets grade 3 (GNP 3) was significantly decreased after weathering in 100% CO_2 gas for a week. This result explains the reason that the RCFI of carbon nanomaterials was increased after heating. The activated carbon or active sites in pristine carbon nanomaterials which can donate the electrons would have been blocked by the CO_2 absorbed on the surface. However, the CO_2 would be released from the surface when the carbon nanomaterials were heated.

For this reason, the heating caused the RCFI increase of carbon nanomaterials in any gas atmospheres as shown in Fig. 12 above. On the other hand, the RCFI of heated GNP 3 was not increased because its surface was largely free of absorbed CO_2. Thus, the RCFI of GNP_3 had been decreased after weathering in pure CO_2 because of CO_2 adsorption. Fig. 25 also shows that the RCFI of GNP 3 weathered in CO_2 was decreased more after weathering in moist synthetic air. This result coincides with the previous result that the RCFI of pristine carbon nanomaterials was significantly decreased after weathering in moist synthetic air. And this result proves that the pristine carbon nanomaterials contain some amount of CO_2 on their surface.

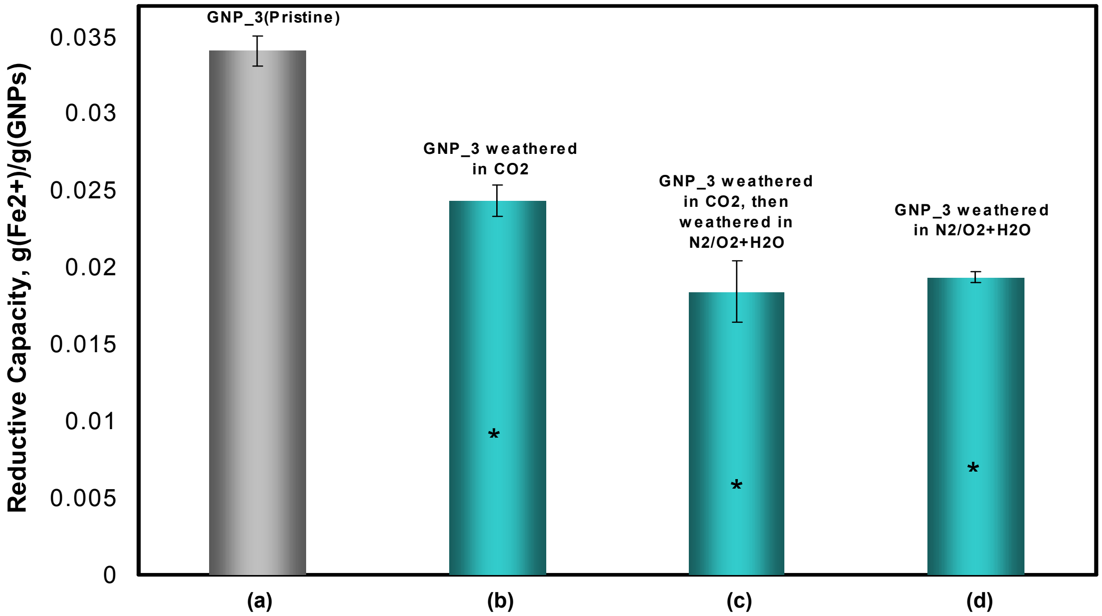

Fig. 25. RCFI of graphene nanoplatelets 3 weathered in CO_2 for blocking effect.
(a) pristine GNP_3 (b) GNP_3 weathered in 100% CO_2 gas (c) GNP_3 weathered in CO_2 then weathered in moist synthetic air (d) GNP_3 weathered in moist synthetic air
'*' means significantly different from pristine sample according to the ANOVA (p: 0.05).
Error bar indicates standard deviation.

3.4.6 RCFI of Carbon Black Weathered in Still Moist Air in Various Times

Weathering in still moist air up to 4 weeks did not cause a significant RCFI change of carbon black. As shown in Fig. 26 (a), the RCFI of carbon black was significantly decreased after 2 weeks of weathering in water bath. However, there was no more decrease after 3 and 4 weeks of weathering.

The weight after weathering was also measured to determine the mass of absorbed water, as shown in Table 11. The mass of absorbed water after one week was only about 5.8% of carbon black mass. However, the mass of absorbed water after 2 weeks was increased critically. And the mass of sandwich sample was increased by 30% after one month of weathering. For this reason, the RCFI of weathered carbon black was calculated again by subtracting the mass of absorbed water. Table 12 and Fig. 26 (b) indicate that the RCFI decrease of weathered carbon black were not significant, and the RCFI was similar to the RCFI of pristine carbon black after subtracting the absorbed water mass.

Table 11. Mass of absorbed water after weathering in still moist air

Time	Mass of sandwich samples before weathering (mg)	Mass of sandwich samples after weathering (mg)	Mass of absorbed water(mg)
1 week	110	116.4	6.4
2 week	110	134.9	24.9
3 week	110	138.5	28.5
4 week	110	142.0	32.0

Table 12. RCFI of carbon black weathered in still moist air subtracting mass of absorbed water

Time	RCFI of weathered carbon black before subtraction(g/g)	RCFI of weathered carbon black after subtraction (g/g)	RCFI differences (g/g)
1 week	9.313×10^{-3}	10.196×10^{-3}	0.883×10^{-3}
2 week	7.116×10^{-3}	9.023×10^{-3}	1.907×10^{-3}
3 week	7.085×10^{-3}	9.329×10^{-3}	2.244×10^{-3}
4 week	6.871×10^{-3}	9.377×10^{-3}	2.506×10^{-3}

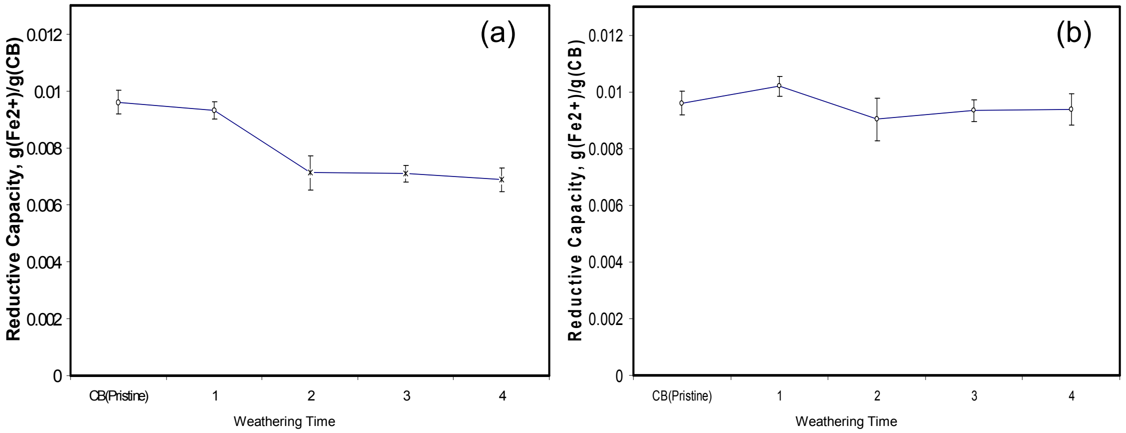

Fig. 26. RCFI of carbon black weathered in still moist air in various weathering times. (a) RCFI of carbon black weathered in still moist air before subtracting absorbed water mass (b) RCFI of carbon black weathered in still moist air after subtracting absorbed water mass

'*' means significantly different from pristine sample according to the ANOVA (p: 0.05).
Error bar indicates standard deviation.

3.4.7 RCFI of Carbon Black Weathered in Grazing Moist Synthetic Air

As shown in Fig. 27, the RCFI of carbon black was not significantly decreased after a week of weathering in still moist air (room air, CO_2-containing). Also, the RCFI of carbon black was not significantly decreased when the carbon black was weathered in grazing moist synthetic air and CO_2. However, there was significant RCFI decrease when the carbon black was weathered in grazing moist synthetic air. This indicates that the small amount of CO_2 can inhibit the aging effect of O_2. The CO_2 gas in the water bath in still moist air would have interrupted the aging of the carbon black in the same way of moist synthetic air and CO_2 flow. This result shows the reason why the RCFI of carbon black was not decreased after a month of weathering in still moist air above.

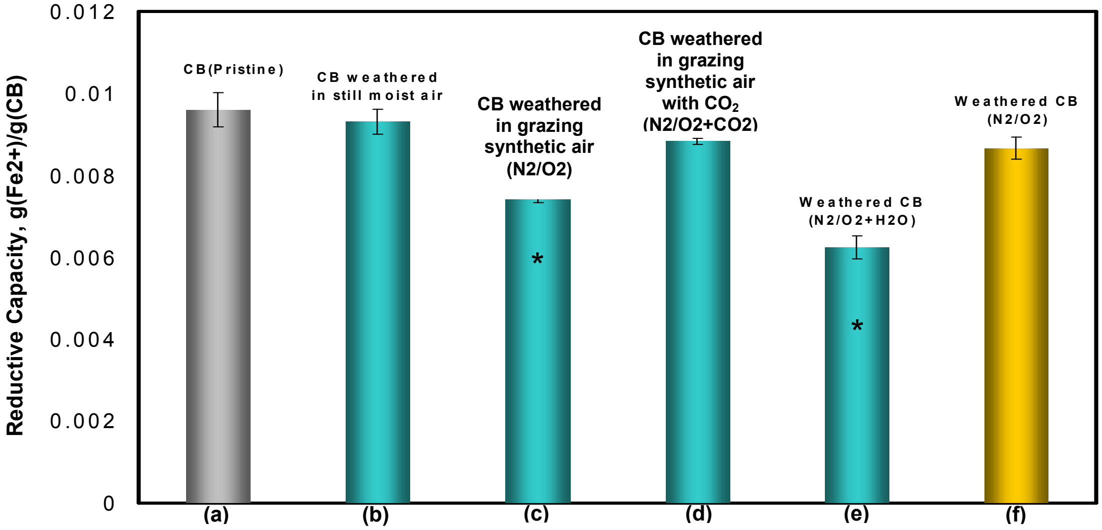

Fig. 27. RCFI of carbon black weathered in grazing moist synthetic air. (a) pristine CB (b) CB weathered in still moist air (c) CB weathered in grazing moist synthetic air (d) CB weathered in grazing moist synthetic air and CO_2 (e) CB weathered in moist synthetic air (f) CB weathered in synthetic air

'*' means significantly different from pristine sample according to the ANOVA (p: 0.05).
Error bar indicates standard deviation.

3.4.8 RCFI of Carbon Black Weathered in Still Air with Different Lighting Conditions

Three pairs of carbon black samples were weathered in petri dishes as shown in Fig. 9 to determine the effect of light exposure on the weathering of carbon nanomaterials. As shown in Fig. 28, the RCFI of carbon black particles did not change until 2 months of weathering. The RCFI of carbon black was decreased after 3 months of weathering, but the change was not significant. The RCFI of carbon black which was not covered and exposed to the light was decreased more than that of covered carbon black. This indicates that the light exposure may be a significant factor which affects on aging, such that the RCFI of carbon black would be significantly decreased after a long time of weathering more than 3 months if it is exposed to the light.

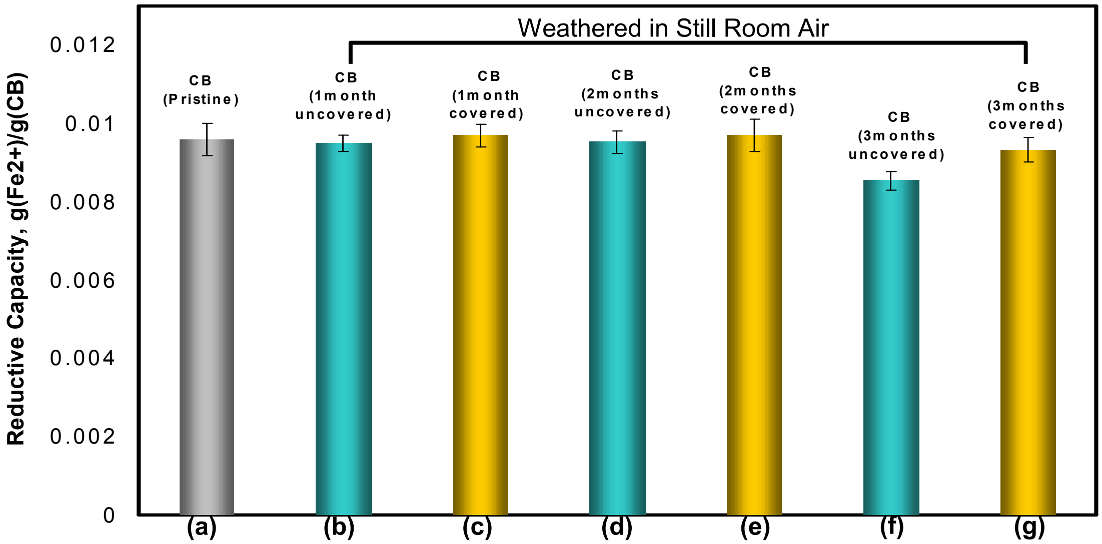

Fig. 28. RCFI of carbon black weathered in still air with different lighting conditions. (a) pristine CB (b) uncovered CB weathered for 1 month (c) covered CB weathered for 1 month (d) uncovered CB weathered for 2 months (e) covered CB weathered for 2 months (f) uncovered CB weathered for 3 months (g) covered CB weathered for 3 months

3.4.9 Diffusion Time Calculation for Weathering Treatment

The diffusion time was determined by calculating the aforementioned diffusion coefficient. In the equation (2) above, radius of an equivalent void (r) needed to be found in order to determine the Knudsen Diffusion Coefficient ($D\kappa$).

Porosity of carbon black was found to be 14 to 18% in Lamond et al [20]. If 14% porosity is assumed for the maximum diffusion time calculation, porosity volume (Vp) of $1cm \times 1cm \times 0.1cm$ volume of carbon black particles would be

$$Vp = 0.1cm^3 \times 0.14 = 0.014cm^3 \tag{3}$$

Degussa carbon black particle diameter was provided by the manufacturer as 14nm. Volume of one Degussa carbon black particle (Vc) would be

$$Vc = \frac{4\pi}{3}(7 \times 10^{-7} cm)^3 = 1.44 \times 10^{-18} (cm^3) \tag{4}$$

Total number of carbon black in $1cm \times 1cm \times 0.1cm$ excluding voids would be

$$Nc = (0.1 - 0.014)cm^3 \div 1.44 \times 10^{-18} cm^3 = 5.97 \times 10^{16} \tag{5}$$

If it is assumed that the same number of spherical voids (Nv) completely fill in porosity volume, the volume of a void (Vv) and radius of a void (r) would be

$$Vv = 0.014cm^3 \div 5.97\times10^{16}cm^3 = \left(\frac{4\pi}{3}\right)r^3\,,\ \ \therefore r = 3.82nm \tag{6}$$

Substituting the value of r into equation (2),

$$D\kappa = \frac{4}{3}\times3.82\times10^{-7}cm\times(2.325cm/s)\left(\frac{(1-0.98)}{2}\right) = 1.1\times10^{-8}cm^2/s \tag{7}$$

$$\frac{1}{D_{eff}} = \frac{1}{D_k}+\frac{1}{D_{12}}\,,\ D_{12}(N_2-O_2) = 0.202cm^2/s\ \ [21] \tag{8}$$

Substituting the value of D_k into equation (8),

$$D_{eff} = 1.1\times10^{-8}cm^2/s \tag{9}$$

Diffusion time scale is defined as

$$T \sim \frac{L^2}{D_{eff}} \tag{10}$$

Accordingly, diffusion time scale for 1mm thickness of carbon black

$$T_1 = \frac{0.1^2}{(1.1 \times 10^{-8})} = 909{,}091 \sec = 15{,}152 \min = 253 hours = 10.5 days$$

The volume of 110mg of carbon black particles contained in a vial was measured as

$$9mm \times 9mm \times 7mm = 567mm^3$$

If 110mg of carbon black particles were dispersed on a 47mm diameter filter paper equally, the thickness (L) would be

$$567mm^3 = \pi(\frac{47mm}{2})^2 \times L\,,\ L = 0.33mm$$

Diffusion time scale for $L = 0.33mm$ would be

$$T_{0.33} = \frac{0.033^2}{(1.1 \times 10^{-8})} = 99{,}000 \sec = 1{,}650 \min = 27.5 hours = 1.2 days$$

According to the diffusion time scale calculation above, diffusion time for 110mg of carbon black particles was calculated as 1.2 days. However, because the thickness of the sample could not be perfectly uniform, the actual diffusion time scale should be longer. The actual thickness of some portions would be thicker or thinner. For this reason, one week of weathering time was used in each treatment to allow for enough diffusion time.

3.5 RCFI of Carbon Nanomaterials after Treatment Cocktails

3.5.1 Carbon Black Heated and Soaked in Water under O_2

Carbon black was heated in air at 200ºC for 2 hours, and then it was soaked in water with O_2 for 2 weeks. Fig. 29 shows that the RCFI of heated carbon black particles was significantly decreased after 2 weeks of soaking in water. It was decreased by 42% compared to the RCFI of heated carbon black. This result indicates that soaking can reduce the RCFI of carbon nanomaterials even after the RCFI of carbon materials was increased by heating treatments. Accordingly, it can be determined that the soaking treatment is the opposite process of heating treatment in terms of the RCFI changes of carbon nanomaterials.

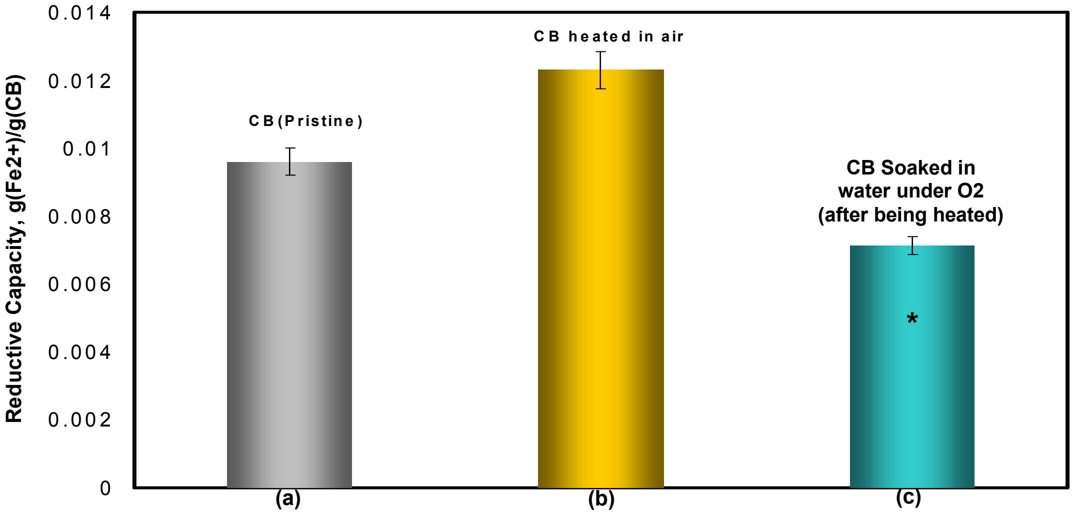

Fig. 29. RCFI of carbon black heated and soaked in water under O_2. (a) pristine CB (b) CB heated 200ºC for 2 hours in air (c) CB heated soaked in water under O_2 for 2 weeks
'*' means significantly different from heated samples according to the ANOVA (p: 0.05). Error bar indicates standard deviation.

3.5.2 Carbon Black Heated and Weathered in Moist Synthetic Air

Carbon black was heated in air at 200ºC for 2 hours, and then it was weathered in moist synthetic air for 1 week. As shown in Fig. 30, the RCFI of heated carbon black was significantly decreased after weathering in moist synthetic air. It was decreased by 29% compared to the RCFI of heated carbon black. This result is in accordance with the result of Fig. 29, that the RCFI of heated carbon black can retrieve its RCFI by weathering treatment.

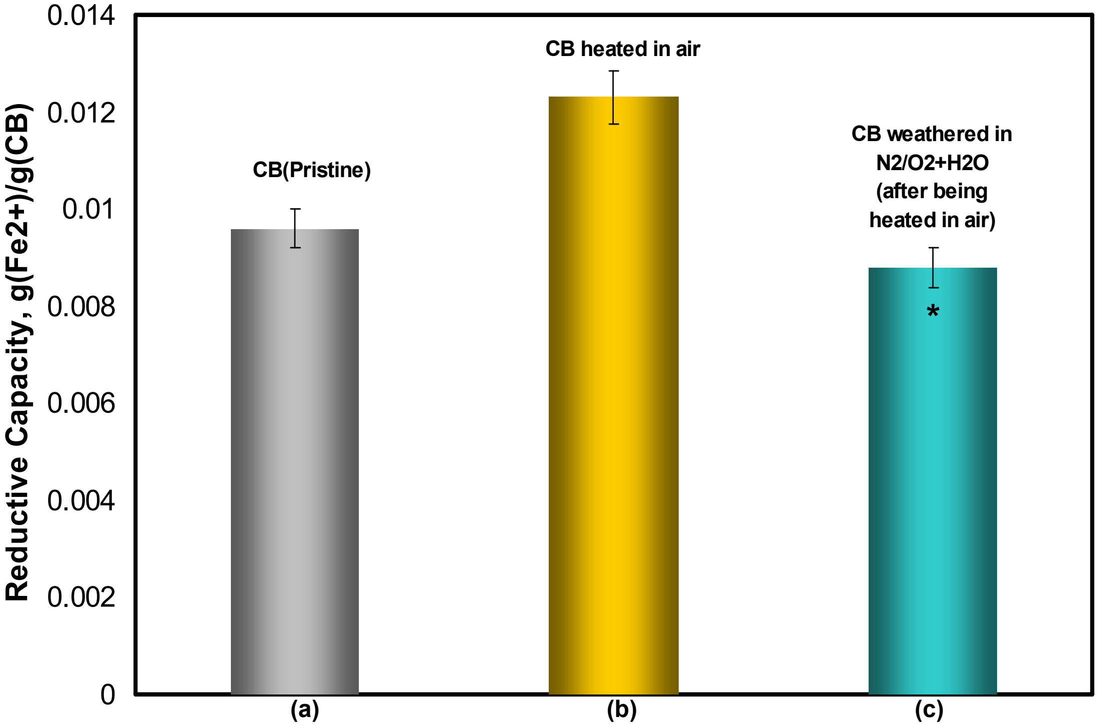

Fig. 30. RCFI of carbon black heated and weathered in moist synthetic air. (a) pristine CB (b) CB heated 200ºC for 2 hours in air (c) CB heated and weathered in moist synthetic air

'*' means significantly different from heated samples according to the ANOVA (p: 0.05). Error bar indicates standard deviation.

3.6 XPS Results and Analysis

3.6.1 XPS Result of Carbon Black

In association with the XPS result, the O_2 high resolution scan of some carbon nanomaterials was not acquired. For those samples, the XPS deconvolution was carried out using the survey scan and the high resolution scan of carbon. Accordingly, it is possible that the XPS deconvolution data may have some inaccuracies.

The XPS result of carbon black in Table 13 shows that the pristine carbon black has a higher surface oxidation than the heated and aged carbon black. A general correlation between surface oxidation and the RCFI could not be found as shown in Table 13. This means that the XPS result can not show the oxidation of the carbon nanomaterials. This is because some carbon may be oxidized to carbon dioxide and released, as found in other studies [19, 22]. Also, there wasn't any general correlation between functional group changes and treatments as shown in Fig. 31. However, the depletion of C-O single bond after aging and the increase of C-O single bond after heating can be found. This result coincides with the other studies that the aging treatment induced the depletion of C-O single bond, and the OH surface functional groups enhance the reduction of Fe^{3+} as explained above [19]. In addition, high adventitious C and COOH (Carboxyl) functional group ratio in high RCFI could be found. Accordingly, adventitious C and COOH functional groups might be related to the reason of the RCFI increase. Thus, it can be determined that the definitive correlation between the oxidation and RCFI changes of carbon black can not be found by the XPS result, but C-O or adventitious C and COOH surface functional groups may have an effect on the RCFI of carbon black.

Table 13. XPS deconvolution result and RCFI of carbon black

Species	CB AW (at. %)	CB AA (at. %)	Pristine CB (at. %)	CB HA (at. %)
RCFI(g/g)	**0.0061**	**0.0062**	**0.0096**	**0.0123**
GRAPHITE	1.32	0.00	0.00	0.00
C=C	74.89	83.48	55.84	64.33
Adventitious C	8.20	5.20	26.34	21.46
C-O	**2.56**	**4.09**	**6.35**	**6.43**
C=O	0.82	0.00	0.50	0.00
COOH	3.97	1.04	7.82	4.94
$\%C_{unox} = [C_{unox} / C_{unox} + C_{ox}]*100$	91.99	94.53	84.85	88.30
$\%C_{ox} = [C_{ox} / C_{unox} + C_{ox}]*100$	**8.01**	**5.47**	**15.15**	**11.70**
$\%C_{ox} : \%C_{unox}$	**0.09**	**0.06**	**0.18**	**0.13**
$\%C_{C\text{-}OH} = [C_{C\text{-}O} / C_{unox} + C_{ox}]*100$	0.03	0.04	0.07	0.07
$\%C_{(O)C=O} = [C_{OC=O} + C_{C=O} / C_{unox} + C_{ox}]*100$	0.05	0.011	0.09	0.05
$\%C_{(O)C=O} : \%C_{C\text{-}OH}$	**1.87**	**0.25**	**1.31**	**0.77**

* HA(Heated in air), AA(Weathered in N_2/O_2 with moisture), AW(Soaked in water with O_2)

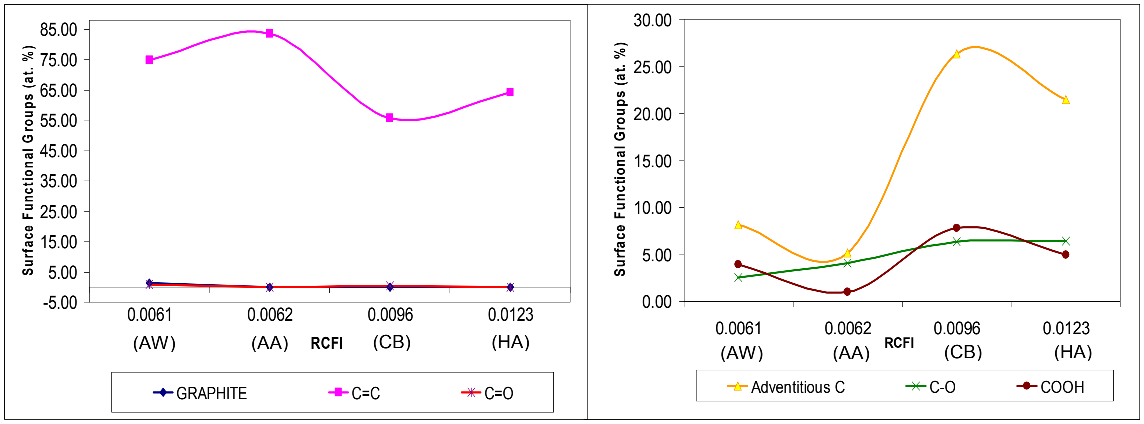

Fig. 31. RCFI of carbon black vs. surface functional group changes

* HA(Heated in air), AA(Weathered in N_2/O_2 with moisture), AW(Soaked in water with O_2)

3.6.2 XPS Result of Graphene Nanoplatelets

As shown in Table 14, we couldn't find any general correlation between the oxidation and RCFI changes of graphene nanoplatelets after heating and aging treatments by XPS result. This XPS result of GNPs strengthens the result that there is no correlation between oxidation and oxygen functional group changes of carbon nanomaterials. In addition, Fig. 32 shows that the oxygen-containing functional group changes of GNPs do not have any proportional relation with the RCFI changes of GNPs after treatments. Also, it was dissimilar with the XPS result of carbon black that any correlation could not be found between C-O single bond and RCFI changes of GNPs. This means that the RCFI changes of carbon nanomaterials after treatments mainly originated from other factors rather than the oxygen-containing surface functional group changes.

Table 14. XPS deconvolution result and RCFI of graphene nanoplatelets

Species	**GNP_1 AA (at. %)**	**GNP_1 (at. %)**	**GNP_1 HA (at. %)**	**GNP_2 AW (at. %)**	**GNP_2 AA (at. %)**	**GNP_2 (at. %)**	**GNP_2 HA (at. %)**	**GNP_3 AW (at. %)**	**GNP_3 AA (at. %)**	**GNP_3 (at. %)**	**GNP_3 HA (at. %)**
RCFI(g/g)	**0.0036**	**0.0065**	**0.0080**	**0.0057**	**0.0078**	**0.0104**	**0.0127**	**0.0176**	**0.0193**	**0.0340**	**0.0311**
GRAPHITE	2.61	2.57	1.26	4.20	1.16	2.12	2.71	0.56	1.12	0.00	0.00
C=C	83.52	84.13	82.91	82.89	74.03	84.18	83.63	75.93	78.31	72.80	71.90
Adventitious C	3.84	4.04	5.05	4.02	9.13	6.99	4.47	11.46	7.49	10.88	10.39
C-O	2.59	2.55	2.42	2.51	2.18	2.16	1.59	3.48	2.15	2.35	4.89
C=O	1.03	0.66	1.00_	0.05	1.93	0.57	0.11	1.86	0.46	1.22	3.35
COOH	0.75	0.46	1.49	0.72	1.55	0.71	0.73	1.52	0.66	1.25	2.05
$\%C_{unox} = [C_{unox}/C_{unox}+C_{ox}]*100$	95.37	96.11	94.78	96.53	93.71	96.44	97.39	92.76	96.37	94.55	88.89
$\%C_{ox} = [C_{ox}/C_{unox}+C_{ox}]*100$	**4.63**	**3.89**	**5.22**	**3.47**	**6.29**	**3.56**	**2.61**	**7.24**	**3.63**	**5.45**	**11.11**
$\%C_{ox} : \%C_{unox}$	**0.05**	**0.04**	**0.06**	**0.04**	**0.07**	**0.04**	**0.03**	**0.08**	**0.04**	**0.06**	**0.13**
$\%C_{C\text{-}OH} = [C_{C\text{-}O}/C_{unox} + C_{ox}]*100$	0.03	0.03	0.03	0.03	0.02	0.02	0.02	0.04	0.02	0.03	0.05
$\%C_{(O)C=O} = [C_{OC=O} + C_{C=O}/C_{unox}+C_{ox}]*100$	0.02	0.01	0.03	0.01	0.04	0.01	0.01	0.04	0.01	0.03	0.06
$\%C_{(O)C=O} : \%C_{C\text{-}OH}$	**0.69**	**0.44**	**1.03**	**0.31**	**1.60**	**0.59**	**0.53**	**0.97**	**0.52**	**1.05**	**1.10**

* HA(Heated in air), AA(Aged in N_2/O_2 with moisture), AW(Aged in water with O_2)

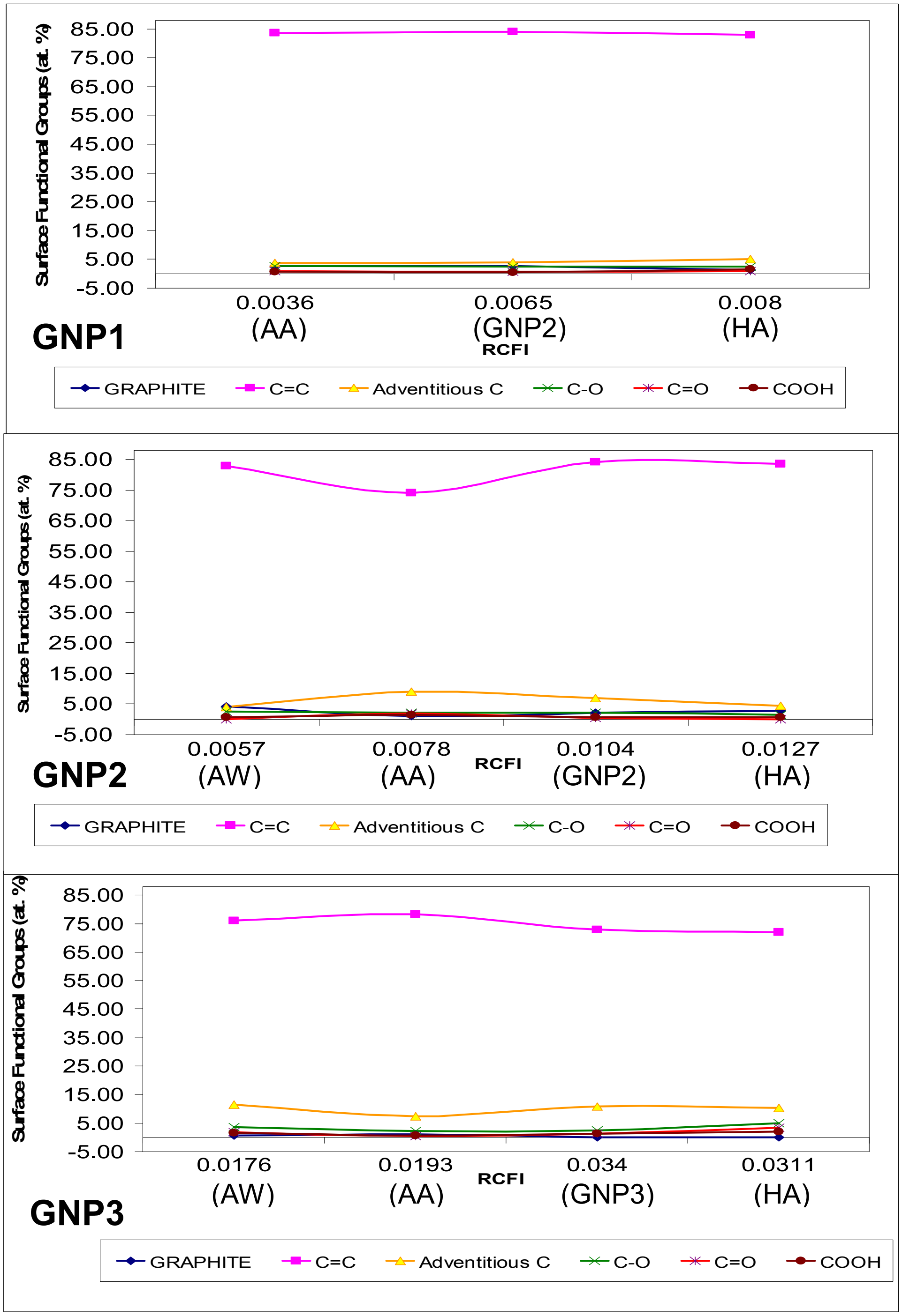

Fig. 32. RCFI of GNPs vs. surface functional group changes

* HA(Heated in air), AA(Weathered in N_2/O_2 with moisture), AW(Soaked in water with O_2)

4. DISCUSSION

The RCFI was not proportional to specific surface area. This suggests that RCFI is related to surface sites that are reactive towards Fe^{3+}; the density of such reactive sites on the surface apparently depends on the carbon nanomaterial

The reason for the RCFI increase of carbon nanomaterials after heating may be explained by the release of CO_2 from the surface which is blocking the reactive surface sites. The CO_2 desorption from activated carbon at temperatures raging from 440K to 870K was revealed by Haydar et al. In Haydar et al., the temperature-programmed desorption (TPD) apparatus was used under vacuum to obtain the CO_2 desorption spectra of activated carbon [23].

Aging by O_2 led to significant RCFI decreases. The result may be explained by the decrease of reactive surface sites. Aging by O_2 in the presence of water vapor caused decrease of RCFI more than aging by O_2. Also, the RCFI of carbon nanomaterials was increased more when the carbon nanomaterials were heated with moisture. This indicates that the water vapor can enhance the RCFI decrease in aging and the RCFI increase in heating. According to the Petit et al, water vapor reacts with activated carbon evolving CO_2 at 150ºC, and this reaction was due to the hydrolysis reaction or water-catalysed decomposition of some oxygenated groups [24]. Thus, the RCFI increase in heating would be derived from the CO_2 release by reaction between water vapor and CO_2 in the surface. And the water vapor would be the driving force of aging process which decreased the RCFI by reacting with activated carbon.

Besides, CO_2 had an influence on the RCFI of aged carbon nanomaterials. The RCFI of carbon nanomaterials was less decreased when the carbon nanomaterials were aged in CO_2-containing gas. This indicates that the CO_2 can interrupt the aging effect. The inlet of CO_2 gas of carbon nanomaterials might have interrupted the reaction between active sites and oxygen.

The XPS results of carbon nanomaterials could not reveal a definitive correlation between the oxidation and RCFI changes after aging by O_2. This suggests that we may not be able to quantitatively predict the reductive capacity of carbon nanomaterials. In addition, we could not find a positive proportional relation between the RCFI changes after treatments and the oxygen-containing functional group changes of carbon nanomaterilas. One thing we could find in the XPS result was the proportional increase of C-O single bond as the RCFI increase and the high percentage of adventitious C and COOH in high RCFI, but it was only for the case of carbon black. This indicates that the RCFI changes of carbon nanomaterials after treatments mainly derived from factors other than the oxygen-containing surface functional group changes.

Fu et al. proposed that the reductive capability of activated carbon fibers was mainly related with the edges rather than the surface of the carbon. The oxygen-containing functional groups provide only a small part of the reduction capacity. Many active sites with active hydrogen such as anthracene and phenanthrene participate in redox reaction [19]. Thus, the RCFI decrease of aged carbon nanomaterials would be generally caused by the decrease of active sites of edges and the surface rather than the oxygen-containing functional group changes.

5. SUMMARY AND CONCLUSION

The RCFI of carbon nanomaterials after various engineering treatments was determined as below:

- Heating led to significant increase in RCFI, regardless of the atmosphere.
- Water vapor enhanced the increase of RCFI in the heating treatment; CO_2 did not affect the heating treatment significantly.
- Aging by O_2 resulted in significant decrease in RCFI, either in water or gas atmosphere.
- Water vapor enhanced the RCFI decrease due to weathering in synthetic air. Thus, both O_2 and water are important factors to cause the significant RCFI decrease.
- Small amounts of CO_2 inhibited aging by O_2 in both soaking and weathering.

The correlation between the RCFI changes after various treatments and the oxygen-containing surface functional group changes were studied using XPS. The results are as follows:

- C-O or adventitious C and COOH surface functional groups showed some correlation with RCFI of carbon black.
- The definitive correlation between the RCFI changes after treatments and the oxygen-containing functional group changes couldn't be found.

In conclusion, aging by O_2 led to the RCFI decrease of carbon nanomaterials. The RCFI decrease after aging would be mainly caused by the decrease of reactive sites on the surface. On the other hand, heating led to the RCFI increase of carbon nanomaterials. The RCFI increase after heating is probably due to the release of absorbed CO_2 that would block the reactive sites. Aging by O_2 may decrease the toxicity of carbon nanomaterials while heating may increase the toxicity of carbon nanomaterials.

CO_2 inhibits the aging effect by O_2, but absorbed CO_2 also affects the RCFI. Therefore, environmental concentration of CO_2 may affect the mitigation (or exacerbation) of carbon nanomaterials release into the environment. Finally, this study shows that the RCFI measurement have its own value that can be used to determine reductive capability that is not feasible with XPS measurement.

REFERENCES

[1] Nel A, Xia T, Madler L, Li N. 2006. Toxic potential of materials at the nanolevel. *Science* 311:622-627.

[2] Valko M, Morris H, Cronin MTD. 2005. Metals, toxicity and oxidative stress. *Current Medicinal Chemistry* 12:1161-1208.

[3] Roy DR, Parthasarathi R, Subramanian V, Chattaraj PK. 2006. An electrophilicity based analysis of toxicity of aromatic compounds towards Tetrahymena pyriformis. *Qsar & Combinatorial Science* 25:114-122.

[4] Guo B, Zebda R, Drake SJ, Sayes CM. 2009. Synergistic effect of co-exposure to carbon black and Fe2O3 nanoparticles on oxidative stress in cultured lung epithelial cells. *Particle and Fibre Toxicology* 6:4.

[5] Sacan MT, Cecen F, Erturk MD, Semerci N. 2009. Modelling the relative toxicity of metals on respiration of nitrifiers using ion characteristics. *Sar and Qsar in Environmental Research* 20:727-740.

[6] Munday R. 1988. Generation of Superoxide Radical, Hydrogen-Peroxide and Hydroxyl Radical during the Autoxidation of N,N,N',N'-Tetramethyl-Para-Phenylenediamine. *Chemico-Biological Interactions* 65:133-143.

[7] Cheng CH, Lehmann J. 2009. Ageing of black carbon along a temperature gradient. *Chemosphere* 75:1021-1027.

[8] Yang LC, Kim P, Meyer HM, Agnihotri S. 2009. Aging of nanocarbons in ambient conditions: Probable metastability of carbon nanotubes. *Journal of Colloid and Interface Science* 338:128-134.

[9] Bradley RH, Sutherland I, Sheng E. 1996. Carbon surface: Area, porosity, chemistry, and energy. *Journal of Colloid and Interface Science* 179:561-569.

[10] Desimoni E, Casella GI, Salvi AM. 1992. Xps Xaes study of carbon-fibers during thermal annealing under Uhv conditions. *Carbon* 30:521-526.

[11] Pantea D, Darmstadt H, Kaliaguine S, Roy C. 2003. Heat-treatment of carbon blacks obtained by pyrolysis of used tires. Effect on the surface chemistry, porosity and electrical conductivity. *Journal of Analytical and Applied Pyrolysis* 67:55-76.

[12] Boehm HP. 1994. Some aspects of the surface-chemistry of carbon-blacks and other carbons. *Carbon* 32:759-769.

[13] Drake SJ. 2008. Time-dependent release of iron from soot particles by acid extraction and the reduction of fe3+ by elemental carbon. *Master's thesis*, Texas A&M, College Station, TX.

[14] Beck-Speier I, Dayal N, Karg E, Maier KL, Schumann G, Schulz H, Semmler M, Takenaka S, Stettmaier K, Bors W, Ghio A, Samet JM, Heyder J. 2005. Oxidative stress and lipid mediators induced in alveolar macrophages by ultrafine particles. *Free Radical Bio Med* 38:1080-1092.

[15] Hwang W. 2010. Standardization and application of spectrophotometric method for reductive capacity measurement of nanomaterials. *Master's thesis*, Texas A&M, College Station.

[16] Stanleywood NG, Sirajuddin M. 1982. Knudsen diffusion of various gases through a barium-sulfate packed-bed. *Powder Technology* 33:17-24.

[17] Sherwood PMA. 1984. Surface-analysis in electrochemical studies. *Trac-Trends in Analytical Chemistry* 3:121-125.

[18] Walton J. 2010. Peak fitting with CasaXPS: a Casa pocketbook. Acolyte Science. Knutsford, Cheshire, England, UK

[19] Fu RW, Zeng HM, Lu Y. 1994. Studies on the mechanism of the reaction of activated carbon-fibers with oxidants. *Carbon* 32:593-598.

[20] Lamond TG. 1976. Carbon-Black Porosity .1. Interparticle capillary condensation in pelletized carbon-blacks. *Journal of Colloid and Interface Science* 56:109-115.

[21] Marrero TR, Mason EA. 1980. Temperature-dependence of gaseous-diffusion coefficients. *Chem Eng Commun* 7:159-168.

[22] Medalia AI. 1977. Carbon black. Physics, chemistry and elastomer reinforcement. *Journal of Colloid and Interface Science* 62:195-196.

[23] Haydar S, Moreno-Castilla C, Ferro-Garcia MA, Carrasco-Marin F, Rivera-Utrilla J, Perrard A, Joly JP. 2000. Regularities in the temperature-programmed desorption spectra of CO2 and CO from activated carbons. *Carbon* 38:1297-1308.

[24] Petit JC, Bahaddi Y. 1993. New insight on the chemical role of water-vapor in the aging of activated carbon. *Carbon* 31:821-825.

[25] Newcombe DT, Cardwell TJ, Cattrall RW, Kolev SD. 1999. An optical redox chemical sensor based on ferroin immobilised in a Nafion (R) membrane. *Analytica Chimica Acta* 401:137-144.

[26] Kung KH, Mcbride MB. 1988. Electron-transfer processes between hydroquinone and iron-oxides. *Clay Clay Miner* 36:303-309.

APPENDIX A

CHEMICAL REACTION FOR COLOR DEVELOPMENT

1,-10-Phenanthroline is a polycylclic organic compound which has the molecular formula of $C_{12}H_8N_2$. It is composed of three benzene rings with two nitrogen atoms. When 1,10-phenanthroline meets Fe^{2+} it forms a 'ferroin' which appears in red. This reaction can be described by the following:

$$Fe^{2+} + 3Phen \rightarrow [Fe(Phen)_3]^{2+}, E^o = 1.06V \text{ [25]}$$

1,10-phenanthroline was used as an indicator of Fe^{2+} ion by using the color development in a spectrophotometer.

Hydroquinone is a heterocyclic organic compound with two hydroxyl groups (-OH) bonded to a phenyl ring which has the chemical formula of $C_6H_4(OH)_2$. When Hydroquinone meets Fe^{3+}, it donates electrons and reduces Fe^{3+} to Fe^{2+} by the following reaction:

$$2Fe^{3+} + C_6H_4(OH)_2 \rightarrow 2Fe^{2+} + C_6H_4O_2 + 2H^+ , E^o = 0.071V \text{ [26]}$$

The reduction of Fe^{3+} by hydroquinone would finish when either Fe^{3+} or hydroquinone is completely consumed.

APPENDIX B

RCFI CALCULATION

The RCFI of carbon nanomaterials was calculated by using the calibration curve which was determined in Hwang's thesis [15]. The calibration curve was made by a series of absorbance measurements with Fe^{2+} concentration. After plotting the results, it was found that the absorbance and Fe^{2+} ion concentration (mg/L) has a linear relationship with a slope of 0.1893 [15]. The Fe^{2+} ions concentration (mg/L) in the solution was found by multiplying the slope of the calibration curve (0.1893) to the absorbance difference between flask A and C. And then, the dilution factor (4) and volume of the incubated solution (0.1L) were multiplied to the Fe^{2+} ions concentration in final solution (mg/L) to determine the mass of Fe^{2+} reduced from Fe^{3+} during incubation (mg). Finally, the mass of Fe^{2+} reduced from Fe^{3+} (mg) was divided by the mass of the incubated carbon nanomaterials (mg) to get the RCFI of carbon nanomaterials (g/g). The mean of the RCFI calculated from triplicate samples could be used as the final RCFI of the carbon nanomaterials.

APPENDIX C

EQUIPMENT FOR HEATING AND AGING TREATMENTS

In terms of heating treatments, carbon nanomaterials were heated in a tube furnace (Barnstead international, Dubuque, Iowa, USA). The tube furnace had a quartz tube inside which has 900mm length, 50mm diameter and 3mm thickness. De-ionized (DI) water used for the treatments was obtained via a Millipore Milli-Q and Milli-RO Ultrapure Water Purification System. Glassware and laboratory tools were sonicated, rinsed with DI water, and dried in ambient air before and after treatments. Room temperature was kept at 20 ± 3 ˚C while all experiments were conducted. A HEPA filter (high efficiency particulate air filter, Life Sciences) was used to filter the air flowing through the alumina filter. A humidity meter (HOBO U10, 2006 Onset Computer Corporation) was used to measure the humidity during the weathering treatments in the air filter. A multi gas controller 647C (2004 MKS Instruments Deutschland GmbH) was used for controlling gas flow rate. A stirring plate (610T, Fisher Scientific Inc.) was operated during soaking treatment in water.

APPENDIX D

HEATING TREATMENT SAFETY OPERATION PROCEDURE

(a) Go ‘SPrr’ mode, and set a heating rate. (If using H_2 gas, 5 ^{o}C/min can only be used as the ramping rate)

(b) Set the heating temperature and time. (If needed, change the heating mode, it is normaly set Opt.1). Make sure that the furnace is off.

(c) Place the sample into the furnace.

(d) Make sure the gas tubes are properly connected and both sides are covered well. (Gas cylinder → mass flow controller → furnace)

(e) Set flow rate of each gas, and make sure the mass controller channels are closed.

(f) Open gas cylinder valves. Check the cylinder gauge if the gas is properly flowing.

(g) Turn on each gas and check if the actual flow rate on the mass controller panel is the same as you set. Put the gas tubes into water to see if the gas actually comes out.

(h) Turn off all gases, and connect the gas tubes to the furnace.

(i) Turn on all gases except H_2 first to allow them enough time to fill up the furnace tube.

(j) Turn on the H_2 gas last.

(k) Turn on the furnace. Check that the temperature increases with the correct heating rate.

(l) After heating, wait until the temperature decreases to 50^{o}C with all gases on.

(m) Turn off the gases and close the cylinder valves.

(n) Take the sample out. (Use the insulated gloves in case the temperature is hot)

APPENDIX E

METHOD OF XPS DATA CONVERSION FOR DECONVOLUTION

XPS instrument generates dset or ASCII type files. ASCII files contain only the XY data collected from the analysis. This data is unusable for the reliable quantification. VAMAS format is a designated and pertinent format for the XPS spectrum deconvolution. The Kratos Axis Ultra XPS instrument can output files which adhere to the VAMAS format. In order to output files in this format, the dset file needs to be converted by using the CnvtDSet.exe program. The CnvtDSet.exe program takes a directory of dset files. The dset is the Kratos file set used to set up and execute the analysis. CnvtDSet.exe program converts dset fileset to .kal files, which are tantamount to VAMAS. After opening CnvtDSet program, select the folder containing dset files, and click convert. The dset file set will be converted to .kal files.

VITA

Name: Chunghoon Lee

Address: Texas A&M University, Department of Mechanical Engineering,
3123 TAMU, College Station, TX 77843-3123

Email Address: chunghoonlee276@gmail.com

Education: B.E., Civil Engineering, Korea Military Academy in South Korea, 2006

M.S., Mechanical Engineering, Texas A&M University, 2011